

Sparse factor models of high dimension

Benjamin Poignard*, Yoshikazu Terada†

January 23, 2025

Abstract

We consider the estimation of a sparse factor model where the factor loading matrix is assumed sparse. The estimation problem is reformulated as a penalized M-estimation criterion, while the restrictions for identifying the factor loading matrix accommodate a wide range of sparsity patterns. We prove the sparsistency property of the penalized estimator when the number of parameters is diverging, that is the consistency of the estimator and the recovery of the true zeros entries. These theoretical results are illustrated by finite-sample simulation experiments, and the relevance of the proposed method is assessed by applications to portfolio allocation and macroeconomic data prediction.

JEL classification: C13; C38.

Key words: Penalized M-estimation; Sparse factor loadings; Sparsistency.

1 Introduction

A major difficulty in the multivariate modeling of high-dimensional random vectors is the trade-off between a sufficiently rich parameterized model to capture complex relationships and yet parsimonious enough to avoid over-fitting issues. In light of this trade-off between parsimony and flexibility, factor modeling is a pertinent solution: it aims to summarize the information from a large data set of dimension p through a small number m of variables called factors. The quantity of interest in factor analysis is the variance-covariance matrix

*Osaka University, Graduate School of Economics, 1-7 Machikaneyama, Toyonaka, Osaka 560-0043, Japan; jointly affiliated at Riken AIP. bpoignard@econ.osaka-u.ac.jp.

†Osaka University, Graduate School of Engineering Science, 1-3 Machikaneyama, Toyonaka, Osaka 560-8531, Japan; jointly affiliated at Riken AIP. terada.yoshikazu.es@osaka-u.ac.jp

Σ^* of the vector of observations, which is specified as $\Sigma^* = \Lambda^* M_{FF} \Lambda^{*\top} + \Psi^*$, with the factor loading matrix Λ^* , the variance-covariance of the factors M_{FF} and the variance-covariance of the idiosyncratic errors Ψ^* . Numerous restrictions can be imposed for the sake of identification. Most works devoted to factor models constrain Ψ^* to be diagonal when the dimension p - the number of variables composing the vector of observations - is fixed. Under this constraint, [Anderson and Amemiya \(1988\)](#) derived the large sample properties of the Gaussian-based maximum likelihood (ML) estimator of the factor model. [Bai and Li \(2012\)](#) extended these asymptotic results when p is diverging and proposed different restrictions on Λ^* and M_{FF} . To relax the diagonal constraint on Ψ^* , [Chamberlain and Rothschild \(1983\)](#) developed the notion of approximate factor models, which allows for cross-correlation among the idiosyncratic errors. Under the condition of bounded eigenvalues of Ψ^* non-diagonal, [Bai and Li \(2016\)](#) derived the large sample properties of the Gaussian-based ML factor model estimator when p diverges. The sparse estimation of a non-diagonal Ψ^* was considered by [Bai and Liao \(2016\)](#). Their approach gave rise to the notion of conditionally sparse factor models, in the sense that Ψ^* is a sparse matrix with bounded eigenvalues. Under orthogonal strong factors, they computed the sparse approximate factor estimator, where Λ^* and Ψ^* are jointly estimated while penalizing Ψ^* only through the adaptive Least Absolute Shrinkage and Selection Operator (LASSO) and Smoothly Clipped Absolute Deviation (SCAD) methods, and derived some consistency results. [Poignard and Terada \(2020\)](#) considered a two-step method for estimating a sparse Ψ^* and derived consistency results together with the conditions for support recovery.

On the other hand, the studies on sparse factor models, where many of the entries of Λ^* are exactly equal to zero, have benefited from a limited attention so far. The key identification issue relating to Λ^* is the rotational indeterminacy, where individual factors are only identified up to a rotation, or equivalently, different sparse column orderings in Λ^* may provide an optimal solution, prohibiting any economic interpretation of the estimated factors. This identification issue has hampered the sparse modeling of Λ^* and rendered its interpretation in terms of sparsity intricate. In a recent work, [Uematsu and Yamagata \(2023\)](#) developed a Principal Component Analysis (PCA)-based sparse estimation procedure for Λ^* . Within the weak factor model setting, they specified a column-wise sparse assumption for Λ^* , where sparsity among the k -th column grows as p^{ν_k} for some unknown deterministic value $0 < \nu_k \leq 1$. They proposed the Sparse Orthogonal Factor Regression (SOFAR) estimator, which corresponds to an adaptive LASSO-penalized least squares problem providing both the estimated factor variables and sparse factor loading matrix, but not the estimator of Ψ^* due to the PCA nature of the framework, and showed its consistency and support recovery. Their analysis of

the SOFAR is developed under the assumption of orthogonal factors and the restriction “ $\Lambda^* \top \Lambda^*$ diagonal”. The latter condition may greatly worsen the performances of the SOFAR method once Λ^* does not satisfy this diagonal restriction. This constraint holds when Λ^* satisfies a perfect simple structure, a case where each row of Λ^* has at most one non-zero element, giving rise to a non-overlapping clustering of variables. To illustrate this point, Figure 1a displays the true sparse loading matrix Λ^* that satisfies a near perfect simple structure, thus violating the constraint “ $\Lambda^* \top \Lambda^*$ diagonal” assumed by the SOFAR method. Based on the data generated from a centered Gaussian distribution with variance-covariance $\Sigma^* = \Lambda^* \Lambda^{*\top} + \Psi^*$, Ψ^* diagonal with positive non-zero components, we applied the SOFAR procedure: Figure 1b displays the loading matrix estimated by the SOFAR and highlights the substantial discrepancy between the SOFAR estimator and the true sparse loading matrix. The details relating to the data generating process are described in Section 4. Following the work of Bai and Liao (2016), Daniele et al. (2024) considered the joint estimation of (Λ^*, Ψ^*) based on a Gaussian quasi-ML with a LASSO penalization on Λ^* and derived some consistency results. Freyaldenhoven (2023) proposed a ℓ_1 -rotation criterion and provided some theoretical properties. However, this is a rotation technique only; thus, there is no guarantee that this approach provides a sparse loading matrix. Hirose and Terada (2023) restricted their analysis to the perfect simple structure and proposed the prenet penalty function to suitably recover such a structure.

Another line of research relates to sparse Bayesian factor models. Recent theoretical studies essentially derived from the strong factor framework: Pati et al. (2014) studied posterior contraction rates for variance-covariance estimation under a particular class of continuous shrinkage priors for Λ^* ; Ohn et al. (2024) derived an inferential framework to learn the factor dimensionality and the sparse structure. The applications of the Bayesian approach typically concern gene expression data, as in West (2003).

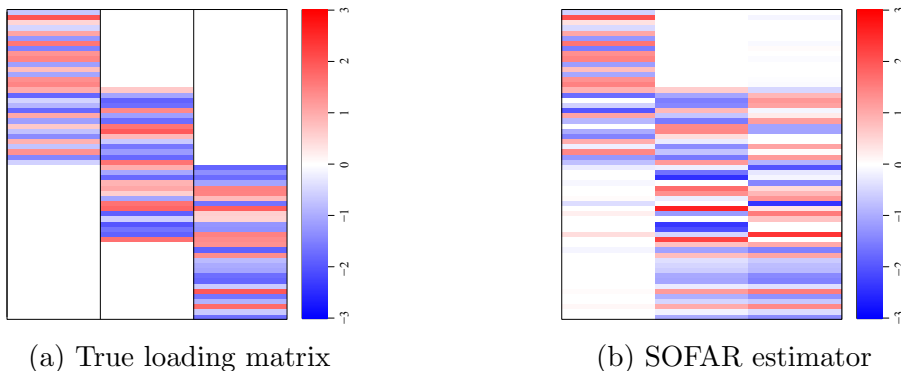


Figure 1: True loading matrix versus SOFAR estimator, with $p = 60$, the number of factors $m = 3$ and sample size $n = 1000$.

In this paper, we aim to tackle the issues previously mentioned for the estimation of potentially any arbitrary sparse Λ^* . We consider the following problem: given n observations of a p -dimensional random vector X_t , we jointly estimate (Λ^*, Ψ^*) while penalizing Λ^* . We first establish the consistency of the factor decomposition-based estimator of Σ^* for any arbitrary sparse Λ^* . Then, under a suitable identification condition, we derive the consistency of Λ^* and Ψ^* , and prove the recovery of the true zero entries of Λ^* . Importantly, our identification restriction on Λ^* allows us to consider the sparsest Λ^* that does not necessarily satisfy the restrictions of [Bai and Li \(2012\)](#) or [Uematsu and Yamagata \(2023\)](#): the latter restrictions may imply sparse loading matrices but may also restrict the diversity of their sparsity patterns. Since the seminal work of [Fan and Li \(2001\)](#), a significant literature on penalized M-estimators has been flourishing: see, e.g., [Fan and Peng \(2004\)](#) for an asymptotic analysis; [Loh and Wainwright \(2015\)](#) or [Poignard and Fermanian \(2022\)](#) for a non-asymptotic viewpoint. In particular, it has been applied to the estimation of variance-covariance and precision matrices of high dimension: e.g., [Rothman et al. \(2008\)](#) derived consistency results for LASSO-penalized precision matrices; [Lam and Fan \(2009\)](#) established the “sparsistency” property of sparse variance-covariance, precision and correlation matrices based on the Gaussian ML, where sparsistency refers to the consistent estimation and the consistent recovery of all the true zero coefficients with probability one. Our proposed estimator for sparse factor models builds upon this framework. Our main contributions are as follows: we develop an estimation procedure for the estimation of sparse factor loading matrix; we prove the consistency and the correct recovery of the true zero entries when the dimension p diverges; we provide an implementation procedure.

The remainder of the paper is organized as follows. [Section 2](#) outlines the sparse factor loading framework. [Section 3](#) is devoted to the asymptotic properties of the penalized factor model estimator. [Sections 4](#) and [5](#) illustrate these theoretical results through simulated and real data experiments. All the proofs of the main text, auxiliary results and implementation details are relegated to the Appendices.

Notations. Throughout this paper, we denote the cardinality of a set E by $|E|$. For $\mathbf{v} \in \mathbb{R}^d$, the ℓ_p norm is $\|\mathbf{v}\|_p = (\sum_{k=1}^d |\mathbf{v}_k|^p)^{1/p}$ for $p > 0$, and $\|\mathbf{v}\|_\infty = \max_i |\mathbf{v}_i|$. For a symmetric matrix A , $\lambda_{\min}(A)$ (resp. $\lambda_{\max}(A)$) is the minimum (resp. maximum) eigenvalue of A , and $\text{tr}(A)$ is the trace operator. For a matrix B , $\|B\|_s = \lambda_{\max}^{1/2}(B^\top B)$ and $\|B\|_F = \text{tr}^{1/2}(B^\top B)$ are the spectral and Frobenius norms, respectively, and $\|B\|_{\max} = \max_{ij} |B_{ij}|$ is the coordinate-wise maximum. For $B \in \mathbb{R}^{p \times m}$, the ℓ_1 matrix norm is $\|B\|_1 = \max_{1 \leq j \leq m} \sum_{i=1}^p |B_{ij}|$. We denote by $O \in \mathbb{R}^{d \times p}$ the $d \times p$ zero matrix. We denote by $\mathcal{O}(m)$ the set of all $m \times m$ orthogonal matrices. $\text{vec}(A) \in \mathbb{R}^{dp}$ is the vectorization operator that

stacks the columns of the matrix $A \in \mathbb{R}^{d \times p}$ on top of one another into a vector. For a square matrix $A \in \mathbb{R}^{d \times d}$, $\text{diag}(A)$ is the operator that stacks the diagonal elements of A on top of one another into a vector. The matrix I_d denotes the d -dimensional identity matrix. For two matrices A, B , $A \otimes B$ is the Kronecker product. For two matrices A, B of the same dimension, $A \odot B$ is the Hadamard product. For a function $f : \mathbb{R}^d \rightarrow \mathbb{R}$, we denote by ∇f the gradient or subgradient of f and $\nabla^2 f$ the Hessian of f . We denote by ∂f the component-by-component partial derivative of f . \mathcal{S}^c denotes the complement of the set \mathcal{S} .

2 The framework

We consider a sequence of a p_n -dimensional random vector $X_t, t = 1, \dots, n$ following the factor decomposition:

$$\forall t = 1, \dots, n, \quad X_t = \Lambda_n^* F_t + \epsilon_t,$$

where $F_t \in \mathbb{R}^m$ is the vector of factors, $\Lambda_n^* = (\lambda_1^*, \dots, \lambda_{p_n}^*)^\top \in \mathbb{R}^{p_n \times m}$ is the loading matrix, with $\lambda_j^* = (\lambda_{j1}^*, \dots, \lambda_{jm}^*)^\top \in \mathbb{R}^m, j = 1, \dots, p_n$, and $\epsilon_t \in \mathbb{R}^{p_n}$ is the vector of idiosyncratic errors. Both F_t, ϵ_t are not observable; X_t only is observable. Throughout the paper, the number of factors m remains fixed; the sequence (p_n) could tend to the infinity with n , i.e., $p_n \rightarrow \infty$ as $n \rightarrow \infty$. This motivates the indexing of the parameters by n . We make the following assumptions concerning the random variables $(F_t), (\epsilon_t)$.

Assumption 1. (i) $(F_t, \epsilon_t)_{t \geq 1}$ is stationary and ergodic with $\forall 1 \leq j \leq p_n, \mathbb{E}[\epsilon_{t,j}] = 0$, and $\mathbb{E}[\epsilon_t \epsilon_t^\top] = \Psi_n^* \in \mathbb{R}^{p_n \times p_n}$ diagonal with positive diagonal elements $(\sigma_1^{*2}, \dots, \sigma_{p_n}^{*2})$, and $\forall 1 \leq j \leq m, \mathbb{E}[F_{t,j}] = 0, \mathbb{E}[F_t F_t^\top] = M_{FF} \in \mathbb{R}^{m \times m}$, and $\mathbb{E}[\epsilon_t F_t^\top] = O \in \mathbb{R}^{p_n \times m}$.

(ii) $\exists r_1, r_2 > 0, b_1, b_2 > 0$ such that for any $s > 0$:

$$\forall 1 \leq j \leq p_n, \mathbb{P}(|\epsilon_{t,j}| > s) \leq \exp(-(s/b_1)^{r_1}), \quad \forall 1 \leq j \leq m, \mathbb{P}(|F_{t,j}| > s) \leq \exp(-(s/b_2)^{r_2}).$$

Assumption 2. $\exists r_3 > 0$ and $L > 0$ satisfying, for all $n \in \mathbb{Z}^+$: $\alpha(n) \leq \exp(-Ln^{r_3})$, with $\alpha(\cdot)$ the mixing coefficient: $\alpha(n) = \sup_{A \in \mathcal{F}_{-\infty}^0, B \in \mathcal{F}_n^\infty} |\mathbb{P}(A)\mathbb{P}(B) - \mathbb{P}(A \cup B)|$, where $\mathcal{F}_{-\infty}^0, \mathcal{F}_n^\infty$ the filtrations generated by $\{(F_t, \epsilon_t) : -\infty \leq t \leq 0\}$ and $\{(F_t, \epsilon_t) : n \leq i \leq \infty\}$.

Assumptions 1–2 relate to the probabilistic properties of the factors and idiosyncratic errors. Both factors and idiosyncratic errors are allowed to be weakly dependent and to satisfy the strong mixing condition and exponential tail bounds. In particular, in Assumption 1, we assume that the elements of ϵ_t are uncorrelated. This will facilitate the

analysis under high-dimension. This restriction is also stated in Assumption B of [Bai and Li \(2012\)](#).

From Assumptions [1](#), $\mathbb{E}[X_t] = 0$ and the implied variance-covariance $\Sigma_n^* := \text{Var}(X_t)$ becomes $\Sigma_n^* = \Lambda_n^* M_{FF} \Lambda_n^{*\top} + \Psi_n^*$. For the sake of interpreting sparsity which will be our core motivation, we assume the orthogonal factor model, i.e., $M_{FF} = I_m$. This is a standard restriction to avoid some of the indeterminacy issues in factor models: see, e.g., [Anderson \(2003\)](#). If we consider the oblique factor model, we may desire sparsity even for the factor covariance M_{FF} , thus complicating the problem formulation and the theoretical analysis. In light of the diverging nature of the parameters, the problem consists of a sequence of parametric factor models $\mathcal{P}_n := \{\mathbb{P}_{\theta_n}, \theta_n \in \Theta_n := \Theta_{n\Lambda} \times \Theta_{n\Psi}\}$, with $\Theta_n \subseteq \mathbb{R}^{p_n m} \times]0, \infty[^{p_n}$, $\theta_n = (\theta_{n\Lambda}^\top, \theta_{n\Psi}^\top)^\top$, with $\theta_{n\Lambda} = \text{vec}(\Lambda_n)$, $\theta_{n\Psi} = \text{diag}(\Psi_n) = (\sigma_1^2, \dots, \sigma_{p_n}^2)^\top$. Therefore, the number of unknown parameters $p_n(m+1)$ may vary with the sample size. We assume that \mathcal{P}_n contains the ‘‘pseudo-true’’ factor model parameter $\theta_n^* = (\theta_{n\Lambda}^{*\top}, \theta_{n\Psi}^{*\top})^\top$.

Because of the rotational indeterminacy, even under the orthogonal factor model, the model can be identified up to a rotation matrix, and at least m^2 restrictions are required for the sake of identification. Indeed, for any $R \in \mathcal{O}(m)$, $\Lambda_n^* \Lambda_n^{*\top} = \tilde{\Lambda}_n^* \tilde{\Lambda}_n^{*\top}$ with $\tilde{\Lambda}_n^* := \Lambda_n^* R$. In other words, we can rotate Λ_n^* without altering the implied variance-covariance structure. Restrictions have thus been proposed to uniquely fix Λ_n^* : see Section 5 of [Anderson and Rubin \(1956\)](#); Section 4 of [Bai and Li \(2012\)](#). To prove the consistent estimation of the factor model parameters and the sparsistency, we will rely on [Anderson and Rubin \(1956\)](#)’s condition which will be formulated in $\Theta_{n\Lambda}$.

To estimate θ_n^* under sparsity, we consider a global loss $\mathbb{L}_n : \mathbb{R}^{n p_n} \times \Theta_n \rightarrow \mathbb{R}$, where $\mathbb{L}_n(\theta_n)$ is evaluated under the parametric factor model \mathcal{P}_n , and we assume that $\mathbb{L}_n(\theta_n)$ is the empirical loss associated to a continuous function $(\ell_n)_{n \geq 1}$ with $\ell_n : \mathbb{R}^{p_n} \times \Theta_n \rightarrow \mathbb{R}$ and that we can write as $\mathbb{L}_n(\theta) = \sum_{t=1}^n \ell_n(X_t; \theta)$. We will consider two functions: the Gaussian loss and the least squares loss, respectively defined as $\ell_n(X_t; \theta) = \text{tr}(X_t X_t^\top \Sigma_n^{-1}) + \log(|\Sigma_n|)$ and $\ell_n(X_t; \theta) = \text{tr}((X_t X_t^\top - \Sigma_n)^2)$. The sparse factor model estimation problem is

$$\hat{\theta}_n \in \arg \min_{(\theta_{n\Lambda}, \theta_{n\Psi}) \in \Theta_{n\Lambda} \times \Theta_{n\Psi}} \mathbb{L}_n(\theta_n) + n \sum_{k=1}^{p_n m} p(|\theta_{n\Lambda, k}|, \gamma_n), \quad (2.1)$$

when such a minimizer exists. $p(x, \gamma_n), x \geq 0$ is a penalty function and γ_n is the regularization parameter. We will consider the coordinate-separable non-convex SCAD and Minimax Concave Penalty (MCP) penalty functions. The SCAD of [Fan and Li \(2001\)](#),

for $a_{\text{scad}} > 2$, is defined as: for every $x \geq 0$,

$$p(x, \gamma) = \gamma x \mathbf{1}(x \leq \gamma) + \frac{2a_{\text{scad}}\gamma x - x^2 - \gamma^2}{2(a_{\text{scad}} - 1)} \mathbf{1}(\gamma < x \leq a_{\text{scad}}\gamma) + \frac{1}{2}(a_{\text{scad}} + 1)\gamma^2 \mathbf{1}(x > a_{\text{scad}}\gamma),$$

where $a_{\text{scad}} > 2$. The MCP due to [Zhang \(2010\)](#) is defined for $b_{\text{mcp}} > 0$ as: for every $x \geq 0$,

$$p(x, \gamma) = \left(\gamma x - \frac{x^2}{2b_{\text{mcp}}}\right) \mathbf{1}(x \leq b_{\text{mcp}}\gamma) + \gamma^2 \frac{b_{\text{mcp}}}{2} \mathbf{1}(x > b_{\text{mcp}}\gamma).$$

Throughout the paper, we will work under the following assumption, where we require the uniqueness of θ_n^* only.

Assumption 3. $\forall n$, Θ_n is a borelian subset of $\mathbb{R}^{p_n(m+1)}$. The function $\theta_n \mapsto \mathbb{E}[\ell_n(X_t; \theta_n)]$ is uniquely minimized on Θ_n at θ_n^* , and an open neighborhood of θ_n^* is contained in Θ_n .

3 Asymptotic properties

To prove the large sample properties, we make the following assumptions.

Assumption 4. There exists $0 < \kappa < \infty$ large enough such that the true parameter θ_n^* satisfies: (i) $\forall 1 \leq j \leq p_n$, $\|\lambda_j^*\|_2 \leq \kappa$, and (ii) $\forall 1 \leq k \leq p_n$, $\kappa^{-2} \leq \sigma_k^{*2} \leq \kappa^2$.

Assumption 5. For every n , $\Lambda_n^* \in \mathbb{R}^{p_n \times m}$, with m fixed, is s_n -sparse, that is $s_n = \text{card}(\mathcal{S}_n)$ with $\mathcal{S}_n := \{k : \theta_{n\Lambda, k}^* \neq 0, k = 1, \dots, m\}$.

Assumption 6. The map $\theta_n \mapsto \ell_n(X_t; \theta_n)$ is twice differentiable on Θ_n , for every $X_t \in \mathbb{R}^{p_n}$. Any pseudo-true value θ_n^* satisfies the first-order condition $\mathbb{E}[\nabla_{\theta_n} \ell_n(X_t; \theta_n^*)] = 0$.

We will denote by $\partial_1 p(x, \gamma_n)$ (resp. $\partial_{11}^2 p(x, \gamma_n)$) the first order (resp. second order) derivative of $x \mapsto p(x, \gamma_n)$, for any γ_n .

Assumption 7. Define

$$A_n = \max_{1 \leq k \leq p_n m} \{|\partial_1 p(|\theta_{n\Lambda, k}^*|, \gamma_n)|, \theta_{n\Lambda, k}^* \neq 0\}, B_n = \max_{1 \leq k \leq p_n m} \{|\partial_{11}^2 p(|\theta_{n\Lambda, k}^*|, \gamma_n)|, \theta_{n\Lambda, k}^* \neq 0\}.$$

Then we assume $\sqrt{p_n} A_n \rightarrow 0$ and $B_n \rightarrow 0$ as $n \rightarrow \infty$. Moreover, $\exists \bar{K}_1, \bar{K}_2$ finite constants such that $|\partial_{11}^2 p(\theta_1, \gamma_n) - \partial_{11}^2 p(\theta_2, \gamma_n)| \leq \bar{K}_2 |\theta_1 - \theta_2|$ for any real θ_1, θ_2 such that $\theta_1, \theta_2 > \bar{K}_1 \gamma_n$.

Assumption 4 ensures that all the eigenvalues of the factor decomposition-based $\Sigma_n^* = \Lambda_n^* \Lambda_n^{*\top} + \Psi_n^*$ are bounded away from 0 and that $\|\Sigma_n^{*-1}\|_s = O(1)$. The sparsity condition specified in Assumption 5 implies $\|\Lambda_n^{*\top} \Lambda_n^*\|_s \leq \|\Lambda_n^*\|_F^2 = s_n$, $\|\Lambda_n^*\|_1 \leq \sqrt{p_n} \|\Lambda_n^*\|_F =$

$O(\sqrt{p_n s_n})$ and $\|\Lambda_n^*\|_1 \geq \|\Lambda_n^*\|_s = O(\sqrt{s_n})$. The strong factor model condition sets $s_n = p_n$: see, e.g., Assumption 3.5 in [Fan et al. \(2011\)](#) or Assumption 3.3 in [Bai and Liao \(2016\)](#). In contrast, the weak factor model viewpoint entails $s_n = p_n^\nu$ with $\nu \leq 1$: in Assumption A2 in [Bai and Ng \(2023\)](#), $\nu \in]0, 1]$, whereas Assumption 1 in [Daniele et al. \(2024\)](#) sets $\nu \in]1/2, 1]$; the latter work uses the QML framework and thus requires $\nu > 1/2$ for consistent estimation, whereas that work builds upon the PCA framework. Our approach for the consistent estimation of the factor model-based Σ_n^* in [Theorem 3.1](#) and for the sparsistency property in [Theorem 3.2](#) under [Anderson and Rubin \(1956\)](#)'s condition for identification below does not require any specific behavior for s_n other than $s_n = O(p_n)$. However, to prove the consistency of the GLS estimator of the latent factor variables, we will work in the matrix space $\{\Lambda_n \in \mathbb{R}^{p_n \times m} \mid \underline{\mu} \leq \lambda_{\min}(p_n^{-\nu} \Lambda_n^\top \Lambda_n) \leq \lambda_{\max}(p_n^{-\nu} \Lambda_n^\top \Lambda_n) \leq \bar{\mu}\}$ with $\underline{\mu}, \bar{\mu} > 0$ and $\nu \in]1/2, 1]$, a space that includes the weak factor case. This will be helpful to obtain $\|(\Lambda_n^\top \Psi_n^{-1} \Lambda_n)^{-1}\|_s = O_p(p_n^{-\nu})$. [Assumption 6](#) concerns the regularity of the loss function. [Assumption 7](#) relates to regularity of the penalty function and tuning parameter.

The following result establishes the existence of a consistent estimator of the factor model-based variance-covariance.

Theorem 3.1. *Suppose $3r_1^{-1} + 1.5r_2^{-1} + r_3^{-1} > 1$. Let $\rho^{-1} = 3r_1^{-1} + 1.5r_2^{-1} + r_3^{-1} + 1$. Assume $\log(p_n)^{6/\rho} = o(n)$ holds and [Assumptions 1-7](#) are satisfied. Then there exists a sequence of estimators $\hat{\Sigma}_n = \hat{\Lambda}_n \hat{\Lambda}_n^\top + \hat{\Psi}_n$ as defined in [\(2.1\)](#) satisfying*

$$\|\hat{\Sigma}_n - \Sigma_n^*\|_F = O_p\left(p_n \sqrt{\frac{s_n \log(p_n)}{n}} + \sqrt{p_n} A_n\right).$$

To ensure the uniqueness of the factor decomposition for the true covariance matrix, which will allow us to deduce the consistency of $\hat{\theta}_n$ and the sparsistency property, we rely on the following identification condition.

Assumption 8. *[Anderson and Rubin \(1956\)](#)'s condition: For $j = 1, \dots, p_n$, let $\Lambda_{n,-j}^*$ be the matrix obtained by removing the j -th row from Λ_n^* . Assume that there exists a positive constant $c_L > 0$ such that, for each $j = 1, \dots, p_n$, $\Lambda_{n,-j}^*$ contains two submatrices whose determinants are bounded below by c_L .*

The factor loading matrix is not uniquely determined due to the rotational indeterminacy. Here, we assume that the sparsest true loading matrix Λ_n^* satisfies the condition for identification introduced by [Anderson and Rubin \(1956\)](#), for which the upper square

matrix of the sparsest loading matrix Λ_n^* is lower triangular, i.e., denoting $\Lambda_{l,:} \in \mathbb{R}^{l \times m}$:

$$\Lambda_n = \begin{pmatrix} \Lambda_{m,:} \\ \Lambda_{p_n-m,:} \end{pmatrix} \quad \text{with} \quad \Lambda_{m,:} = \begin{pmatrix} \lambda_{11} & 0 & \cdots & 0 \\ \lambda_{21} & \lambda_{22} & \cdots & 0 \\ \vdots & \vdots & \ddots & \vdots \\ \lambda_{m1} & \lambda_{m2} & \cdots & \lambda_{mm} \end{pmatrix} \quad \text{and} \quad \lambda_{ii} > 0 \quad (i = 1, \dots, m). \quad (3.1)$$

The positivity of the diagonal elements is needed to avoid the sign indeterminacy. Since the loading matrix in Figure 1a does not satisfy this condition, one might think that the condition is not suitable for sparse estimation. With a certain variable ordering, even a perfect simple structure may not satisfy $\lambda_{jj} > 0$ for some j . However, it is important to note that this identification condition can be slightly relaxed. In fact, if there exists a $p_n \times p_n$ permutation matrix P_n such that the permuted loading matrix $\tilde{\Lambda}_n^* = P_n \Lambda_n^*$ satisfies condition (3.1), then we can eliminate the rotational indeterminacy. Therefore, we employ the following modified identification condition throughout the paper.

Assumption 9. *The parameter space of Λ_n^* is*

$$\Theta_{n\Lambda} = \{\Lambda_n \in \mathbb{R}^{p_n \times m} \mid \exists P_n \in \Pi(p_n); P_n \Lambda_n \text{ satisfies condition (3.1)}\},$$

where $\Pi(p_n)$ is the set of all $p_n \times p_n$ permutation matrices.

We now can establish the consistency of $\hat{\Lambda}_n$ and $\hat{\Psi}_n$ under the conditions of Assumptions 8 and 9 and the recovery of the zero entries of Λ_n^* - ‘‘sparsity property’’ -. We also prove the consistent estimation of the generalized least squares (GLS) estimator $\hat{F}_t = (\hat{\Lambda}_n^\top \hat{\Psi}_n^{-1} \hat{\Lambda}_n)^{-1} \hat{\Lambda}_n^\top \hat{\Psi}_n^{-1} X_t$ of the latent variable F_t , for any $t = 1, \dots, n$. See Section 14.7 of Anderson (2003) for its derivation.

Theorem 3.2. *In addition to the conditions of Theorem 3.1, suppose Assumptions 8 and 9 are satisfied. Let $\hat{\Lambda}_n$ be the estimator for Λ_n^* , which ignores the sign indeterminacy as usual. The estimator $\hat{\theta}_n = (\hat{\theta}_{n\Lambda}^\top, \hat{\theta}_{n\Psi}^\top)^\top$ defined in (2.1) satisfies:*

$$\|\hat{\theta}_n - \theta_n^*\|_\infty = O_p \left(p_n \sqrt{\frac{s_n \log(p_n)}{n}} + \sqrt{p_n} A_n \right).$$

Assume that the penalty function satisfies $\gamma_n^{-1} \lim_{n \rightarrow \infty} \lim_{x \rightarrow 0} \partial_x p(x, \gamma_n) > 0$. Moreover, assume $\gamma_n \rightarrow 0$, $p_n^2 \sqrt{\log(p_n)} A_n = o(\gamma_n \sqrt{n})$ and $\sqrt{n / (p_n^3 s_n \log(p_n))} \gamma_n \rightarrow \infty$. Then with probability tending to one, $\hat{\theta}_{n\Lambda, k} = 0$ for all $k \in \mathcal{S}_n^c$.

In addition to Assumption 9, assume that the factor loading matrix belongs to the space

$\{\Lambda_n \in \mathbb{R}^{p_n \times m} \mid \underline{\mu} \leq \lambda_{\min}(p_n^{-\nu} \Lambda_n^\top \Lambda_n) \leq \lambda_{\max}(p_n^{-\nu} \Lambda_n^\top \Lambda_n) \leq \bar{\mu}\}$ where $\underline{\mu}, \bar{\mu} > 0$ and $\nu \in]1/2, 1]$. Then the GLS estimator $\hat{F}_t = (\hat{\Lambda}_n^\top \hat{\Psi}_n^{-1} \hat{\Lambda}_n)^{-1} \hat{\Lambda}_n^\top \hat{\Psi}_n^{-1} X_t$ of F_t satisfies, for $t = 1, \dots, n$, $\|\hat{F}_t - F_t\| = o_p(1)$.

The consistent estimation of $\hat{\theta}_n$ stated in Theorem 3.2 relies on Anderson and Rubin (1956)'s condition for identification. This restriction allows us to get $\|\hat{\theta}_n - \theta_n^*\|_\infty \leq C_2 u_n$ from $\|\hat{\Sigma}_n - \Sigma_n^*\|_2 \leq C_1 u_n$ established in Theorem 3.1, with $C_1, C_2 > 0$ and $u_n = p_n \sqrt{s_n \log(p_n)/n} + \sqrt{p_n} A_n$: this is due to the ‘‘strong identifiability’’ property of the factor model stated in Lemma 1 and Theorem 1 in Kano (1983), a property ensured by Assumptions 8 and 9. Further details are provided in Section B of the Appendix. The sparsistency property follows from the consistency of $\hat{\theta}_n$ and suitable conditions on $p(\cdot, \gamma_n)$ and γ_n . The consistency of the GLS estimator \hat{F}_t is proved under weak factors.

4 Simulations

This section presents two data generating processes (DGPs). First, we generate the p_n -dimensional random vector X_t based on the DGP:

$$X_t \sim \mathcal{N}_{\mathbb{R}^p}(0, \Sigma_n^*), \text{ with } \Sigma_n^* = \Lambda_n^* \Lambda_n^{*\top} + \Psi_n^*, \text{ for } t = 1, \dots, n, \quad (4.1)$$

with Λ_n^* assumed s_n -sparse, $s_n := |\mathcal{S}_n|$. The sparsity patterns for Λ_n^* are specified as follows:

(i) **Perfect simple structure with non-sparse blocks; Ψ_n^* diagonal**

Λ_n^* satisfies the perfect simple structure for $p_n = 60, 120, 180$ and $m = 3, 4$, and $s_n = p_n$ for any p_n . When $p_n = 60, m = 3$ (resp. $m = 4$), then $p_n m = 180$ (resp. $p_n m = 240$). When $p_n = 120, m = 3$ (resp. $m = 4$), then $p_n m = 360$ (resp. $p_n m = 480$). When $p_n = 180, m = 3$, then $p_n m = 540$.

(ii) **Perfect simple structure with overlaps, non-sparse blocks; Ψ_n^* diagonal**

Λ_n^* satisfies a near perfect simple structure with overlaps for $p_n = 60, 120, 180$ and $m = 3, 4$. We set the number of overlaps as $\lceil 0.5 \times p_n/m \rceil$ in each case. When $p_n = 60, m = 3$ (resp. $m = 4$), then $p_n m = 180$ (resp. $p_n m = 240$) and $s_n = 80$ (resp. $s_n = 84$), where the size of the overlaps is 10 (resp. 8). When $p_n = 120, m = 3$ (resp. $m = 4$), then $p_n m = 360$ (resp. $p_n m = 480$) and $s_n = 160$ (resp. $s_n = 165$), where the size of the overlaps is 20 (resp. 15). When $p_n = 180, m = 3$, then $p_n m = 540$ and $s_n = 240$, where the size of the overlaps is 30.

(iii) **Perfect simple structure with overlaps, sparse blocks; Ψ_n^* diagonal**

Λ_n^* satisfies the same pattern as in (ii), but we randomly replace some non-zero coefficients by zeros such that the ratio of zero coefficients in Λ_n^* is 70%. When $p_n = 60, m = 3$ (resp. $m = 4$), then $p_n m = 180$ (resp. $p_n m = 240$) and $s_n = 54$ (resp. $s_n = 72$). When $p_n = 120, m = 3$ (resp. $m = 4$), then $p_n m = 360$ (resp. $p_n m = 480$) and $s_n = 108$ (resp. $s_n = 144$). When $p_n = 180, m = 3$, then $p_n m = 540$ and $s_n = 162$.

(iv) **General arbitrary sparse structure; Ψ_n^* diagonal**

The zero entries of Λ_n^* are randomly set. When $p_n = 60, m = 3$ (resp. $m = 4$), then $p m = 180$ (resp. $p m = 240$) and $s_n = 27$ (resp. $s_n = 36$).

When $p_n = 120, m = 3$ (resp. $m = 4$), then $p_n m = 360$ (resp. $p_n m = 480$) and $s_n = 54$ (resp. $s_n = 72$). When $p_n = 180, m = 3$, then $p_n m = 540$ and $s_n = 81$.

(v) **General arbitrary sparse structure; Ψ_n^* sparse non-diagonal**

In this final scenario, the sparsity pattern in Λ_n^* is the same as in setting (iv). However, the idiosyncratic error variables are potentially correlated: the true variance-covariance Ψ_n^* is a sparse non-diagonal matrix.

Note that s_n significantly depends on m in (i)-(ii): in (ii), 44% (resp. 35%) of the entries of Λ_n^* are non-zero when $p_n = 60, m = 3$ (resp. $p_n = 60, m = 4$); the non-zero entries represent 15% of all the coefficients of Λ_n^* for any p_n, m , in (iv)-(v). For each sparsity pattern and (p_n, m, n) , we draw two hundred batches of n independent samples from $X_t \sim \mathcal{N}_{\mathbb{R}^p}(0, \Sigma_n^*)$. For each batch, the diagonal elements of Ψ_n^* are simulated in the uniform distribution $\mathcal{U}([0.5, 1])$ for patterns (i)-(iv); in (v), the proportion of zero coefficients in the lower diagonal part of Ψ_n^* is set as 75% and the non-zero entries are generated as the sum of one or more normally distributed variables, so that $\lambda_{\min}(\Psi_n^*) > 0$; the non-zero parameters of Λ_n^* are simulated in $\mathcal{U}([-2, -0.5] \cup [0.5, 2])$. For each dimension setting (p_n, m) , the sample size is $n = 250, 500$.

The second DGP generates the observations X_t according to the time series dynamic:

$$X_t = \Lambda_n^* F_t + \epsilon_t, \text{ for } t = 1, \dots, n, \quad (4.2)$$

where $\epsilon_t \sim \mathcal{N}_{\mathbb{R}^{pn}}(0, \Psi_n^*)$ and $F_{t,k} = \phi_k F_{t-1,k} + \zeta_{t,k}$ for $t = 1, \dots, n, k = 1, \dots, m$, with $\phi_k \sim \mathcal{U}([0.5, 0.85])$, $\zeta_{t,k} \sim \mathcal{N}_{\mathbb{R}}(0, (1 - \phi_k^2))$. The parameters Λ_n^* and Ψ_n^* are generated as in setting (v), DGP (4.1). We also draw two hundred batches of n observations.

The sparsity pattern in Λ_n^* remains identical for all batches and a given DGP, but the non-zero coefficients may have different locations in Λ_n^* for the sparsity patterns (iii)-(v);

under the sparsity patterns (i) and (ii), the location of the non-zero coefficients remains unchanged for all the batches; for all patterns, the cardinality s_n remains unchanged. In setting (v), the proportion of zero entries remains unchanged for all the batches but the non-zero coefficients of Ψ_n^* may have different locations.

For each batch, we apply our sparsity-based method (2.1) for the Gaussian and least squares losses, which will be denoted by SGF (Sparse Gaussian Factor) and SLSF (Sparse Least Squares Factor), respectively, hereafter. We specify $a_{\text{scad}} = 3.7$, a value identified as optimal in Fan and Li (2001) by cross-validated experiments. The MCP parameter is set as $b_{\text{mcp}} = 3.5$, following Section 5 in Loh and Wainwright (2015). The penalized problem is solved by a gradient descent algorithm. For DGP (4.1), we employ a 5-fold cross-validation procedure to tune γ_n ; when the data arises from (4.2) and due to its time-series nature, we employ an “out-of-sample”-based cross-validation procedure: further details on the implementation and the cross-validation procedure can be found in Section D of the Appendix. To emphasize the efficiency of our approach in terms of support recovery and accuracy, we employ the SOFAR estimator, in which case we use the R package “rrpack” of Uematsu and Yamagata (2023).

We report the variable selection performance through the percentage of zero coefficients in Λ_n^* correctly estimated, denoted by C1, and the percentage of non-zero coefficients in Λ_n^* correctly identified as such, denoted by C2. The mean squared error (MSE), defined as $\|\hat{\theta}_{n\Lambda} - \theta_{n\Lambda}^*\|_2^2$, is reported as an estimation accuracy measure. Due to the rotational indeterminacy, we compel the SOFAR estimator to satisfy the specific identification condition to remove this indeterminacy. Thus, the target loading matrix of SOFAR could be different from the sparsest true loading Λ_n^* . More precisely, we compare the loading matrix estimated by SOFAR, denoted by $\hat{\Lambda}_{n,\text{SOFAR}}$, with both the true Λ_n^* and the rotated true $\hat{\Lambda}_{n,\text{SOFAR}}^*$ defined as: $\hat{\Lambda}_{n,\text{SOFAR}}^* := \Lambda_n^* \hat{R}_{\text{SOFAR}}^*$, $\hat{R}_{\text{SOFAR}}^* := \arg \min_{R \in \mathcal{O}(m)} \|\hat{\Lambda}_{n,\text{SOFAR}} - \Lambda_n^* R\|_F^2$. In each table, in the SOFAR’s column, the MSE values compared with $\hat{\Lambda}_{n,\text{SOFAR}}^*$ are reported in the parenthesis. To be precise, for each target of SOFAR, we selected the best values of the regularization coefficient among various values in the sense of MSE.

When the data is generated from DGP (4.1), setting (i), the true factor loading matrix satisfies the orthogonal constraint, i.e., the restriction stated in Uematsu and Yamagata (2023). Thus, in light of Table 1, our proposed method and the SOFAR provide similar performances. In contrast to the perfect simple structure, Λ_n^* generated from settings (ii)–(v) does not satisfy the orthogonal constraint, meaning that $\Lambda_n^* \Lambda_n^{*\top}$ is non-diagonal. Tables 2–4 suggest that the performances of our method are better than the SOFAR in terms of support recovery. From the viewpoint of MSE, it can be noted that our method

outperforms the SOFAR, although the MSE results based on $\widehat{\Lambda}_{n,\text{SOFAR}}^*$ are smaller. However, if we consider the MSE with $\widehat{\Lambda}_{n,\text{SOFAR}}$, the performance of the SOFAR dramatically worsens as the sparsest true loading differs from the orthogonal structure. As detailed in Section 1, this is because the target of the SOFAR is not necessarily the same as the sparsest true loading matrix. Interestingly, when the data is generated based on setting (v), the recovery/MSE performances of our method displayed in Table 5 are comparable to those reported in Table 4: although Ψ_n^* is estimated under the diagonal constraint, the procedure does not suffer from misspecification. In the time-series case (4.2), our approach outperforms the SOFAR method according to Table 6. Although the MSEs are larger compared to the i.i.d. case, the hierarchy in terms of model performances remains unchanged.

Another point worth mentioning is that the Gaussian loss-based estimation provides better performances in terms of MSE compared to the least squares loss, for any sparsity pattern in Λ_n^* . This is in line with the numerical findings of [Fermanian and Poignard \(2024\)](#) related to the sparse estimation of the covariance matrix of the Gaussian copula by SCAD and MCP when the loss is the Gaussian likelihood and the least squares function.

The results displayed in Setting (iv) suggest that the SOFAR performs well in terms of recovery, where the C1 and C2 metrics are similar to our approach. The main reason is that the generated true Λ_n^* are approximately column orthogonal for this Setting (iv). That is, the off-diagonal elements of $\Lambda_n^{*\top} \Lambda_n^*$ are much smaller than its diagonal elements. To illustrate this point, Figure 2 displays two examples relating to Setting (iv), with $n = 1000$ and $p_n = 180$. As displayed in (a, b, c), there are several misspecified elements in the SOFAR estimator when the true loading matrix slightly diverges from the case of being a column orthogonal matrix. On the other hand, as shown in (d), the SOFAR estimator recovers the true zero/non-zero entries almost perfectly when the true Λ_n^* is nearly column orthogonal.

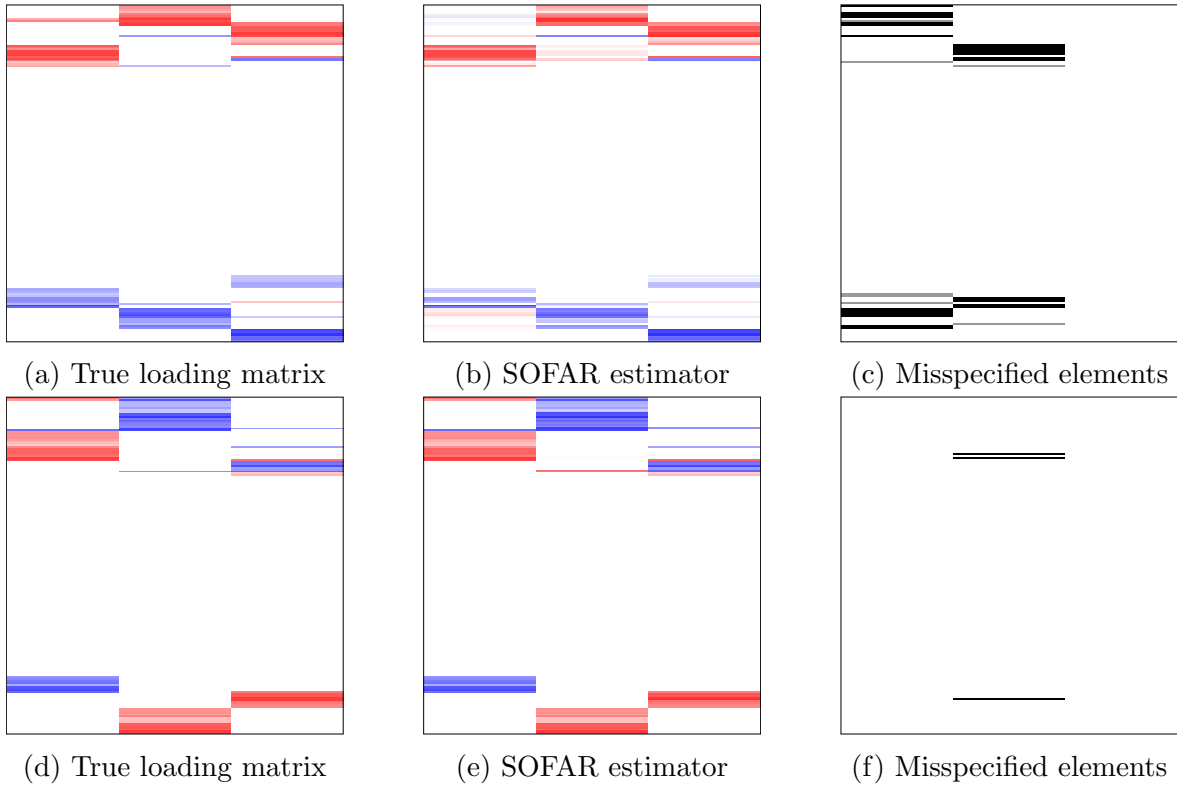


Figure 2: Two examples corresponding to Setting (iv). (a): rearranged true loading matrix; (b): SOFAR estimator for (a); (c) miss-specified elements (black: incorrectly identified non-zero, grey: incorrectly identified zero). (d), (e), (f): alternative example.

Table 1: Model selection and precision accuracy based on 200 replications, DGP (4.1), perfect simple structure without overlaps and non-sparse blocks (sparsity pattern (i)) with respect to (n, p_n, m) .

| (p_n, m) | $n = 250$ | | | $n = 500$ | | | |
|------------|-----------|-----------------|-----------------|-----------------|-----------------|-----------------|-----------------|
| | SGF | SLSF | SOFAR | SGF | SLSF | SOFAR | |
| (60, 3) | C1 | 79.82 – 84.86 | 75.42 – 82.02 | 91.82 | 89.32 – 92.65 | 81.96 – 87.16 | 94.14 |
| | C2 | 100 – 100 | 100 – 100 | 98.39 | 100 – 100 | 100 – 100 | 99.78 |
| | MSE | 0.4588 – 0.4545 | 0.5766 – 0.5797 | 1.6931 (0.6800) | 0.1989 – 0.1978 | 0.2459 – 0.2510 | 0.5738 (0.3060) |
| (60, 4) | C1 | 82.48 – 87.94 | 82.47 – 88.25 | 94.49 | 91.30 – 94.18 | 87.30 – 91.66 | 96.65 |
| | C2 | 100 – 100 | 100 – 100 | 98.03 | 100 – 100 | 100 – 100 | 99.63 |
| | MSE | 0.4751 – 0.4729 | 0.6013 – 0.7343 | 2.0320 (0.8331) | 0.2048 – 0.2036 | 0.2512 – 0.2525 | 0.7455 (0.3679) |
| (120, 3) | C1 | 78.63 – 84.27 | 78.16 – 84.54 | 91.48 | 89.50 – 92.80 | 82.06 – 87.08 | 94.21 |
| | C2 | 100 – 100 | 100 – 100 | 98.01 | 100 – 100 | 100 – 100 | 99.61 |
| | MSE | 0.8781 – 0.8683 | 1.1310 – 1.1321 | 3.9879 (1.4755) | 0.4081 – 0.4050 | 0.5108 – 0.5131 | 1.4386 (0.6683) |
| (120, 4) | C1 | 80.12 – 85.67 | 83.17 – 89.17 | 93.94 | 91.13 – 94.18 | 88.43 – 92.41 | 95.85 |
| | C2 | 100 – 100 | 100 – 100 | 97.41 | 100 – 100 | 100 – 100 | 99.43 |
| | MSE | 0.9378 – 0.9321 | 1.1462 – 1.1482 | 5.0538 (1.8141) | 0.4432 – 0.4395 | 0.5273 – 0.5283 | 1.9252 (0.8381) |
| (180, 3) | C1 | 77.58 – 83.29 | 75.44 – 82.03 | 91.35 | 89.48 – 92.87 | 81.46 – 86.39 | 93.29 |
| | C2 | 100 – 100 | 100 – 100 | 97.91 | 100 – 100 | 100 – 100 | 99.56 |
| | MSE | 1.3781 – 1.3684 | 1.7576 – 1.7638 | 6.2790 (2.3915) | 0.6183 – 0.6144 | 0.7745 – 0.7809 | 2.4009 (1.0297) |

Note: the column “SGF” refers to the estimator deduced from the Gaussian loss with SCAD and MCP penalization, respectively. The column “SLSF” refers to the estimator deduced from the least squares loss with SCAD and MCP penalization, respectively.

The MSE values for SOFAR in parenthesis are based on $\hat{\Lambda}_{n, \text{SOFAR}}^*$, with $\hat{\Lambda}_{n, \text{SOFAR}}^* := \Lambda_n^* \hat{R}_{\text{SOFAR}}^*$, $\hat{R}_{\text{SOFAR}}^* := \arg \min_{R \in \mathcal{O}(m)} \|\hat{\Lambda}_{n, \text{SOFAR}} - \Lambda_n^* R\|_F^2$.

Table 2: Model selection and precision accuracy based on 200 replications, DGP (4.1), perfect simple structure with overlaps and non-sparse blocks (sparsity pattern (ii)) with respect to (n, p_n, m) .

| (p_n, m) | $n = 250$ | | | $n = 500$ | | | |
|------------|-----------|-----------------|-----------------|------------------|-----------------|-----------------|------------------|
| | SGF | SLSF | SOFAR | SGF | SLSF | SOFAR | |
| (60, 3) | C1 | 77.69 – 83.45 | 70.36 – 77.34 | 78.40 | 87.77 – 91.16 | 76.97 – 82.49 | 77.99 |
| | C2 | 100 – 100 | 100 – 100 | 90.29 | 100 – 100 | 100 – 100 | 90.16 |
| | MSE | 0.5901 – 0.5915 | 0.8379 – 0.8507 | 16.4037 (1.0354) | 0.2794 – 0.2781 | 0.4027 – 0.4047 | 15.8031 (0.5070) |
| (60, 4) | C1 | 80.07 – 85.86 | 75.67 – 82.70 | 82.43 | 89.89 – 93.23 | 81.90 – 87.04 | 81.10 |
| | C2 | 100 – 100 | 100 – 100 | 86.42 | 100 – 100 | 100 – 100 | 87.80 |
| | MSE | 0.6667 – 0.6638 | 1.0263 – 1.0450 | 23.8262 (1.3628) | 0.3003 – 0.2989 | 0.4574 – 0.4660 | 24.9719 (0.7080) |
| (120, 3) | C1 | 76.29 – 82.36 | 68.92 – 76.22 | 80.27 | 87.64 – 91.57 | 78.05 – 83.72 | 80.27 |
| | C2 | 100 – 100 | 100 – 100 | 90.65 | 100 – 100 | 100 – 100 | 92.77 |
| | MSE | 1.0821 – 1.0805 | 1.6303 – 1.6473 | 30.6147 (2.0938) | 0.5558 – 0.5543 | 0.7927 – 0.7980 | 23.3241 (1.0257) |
| (120, 4) | C1 | 78.69 – 84.36 | 75.80 – 82.48 | 85.12 | 89.42 – 92.76 | 83.62 – 88.69 | 83.44 |
| | C2 | 100 – 100 | 100 – 100 | 87.18 | 100 – 100 | 100 – 100 | 90.55 |
| | MSE | 1.2606 – 1.2517 | 1.9371 – 1.9716 | 39.1837 (2.8719) | 0.5805 – 0.5776 | 0.8480 – 0.8564 | 34.6621 (1.3524) |
| (180, 3) | C1 | 76.17 – 81.87 | 69.27 – 76.42 | 80.91 | 87.44 – 91.19 | 76.69 – 82.94 | 82.03 |
| | C2 | 100 – 100 | 100 – 100 | 92.01 | 100 – 100 | 100 – 100 | 91.81 |
| | MSE | 1.7192 – 1.7126 | 2.5399 – 2.5583 | 41.5858 (2.9853) | 0.8787 – 0.8771 | 1.2331 – 1.2419 | 37.5806 (1.4952) |

Note: the column “SGF” refers to the estimator deduced from the Gaussian loss with SCAD and MCP penalization, respectively. The column “SLSF” refers to the estimator deduced from the least squares loss with SCAD and MCP penalization, respectively.

The MSE values for SOFAR in parenthesis are based on $\hat{\Lambda}_{n, \text{SOFAR}}^*$, with $\hat{\Lambda}_{n, \text{SOFAR}}^* := \Lambda_n^* \hat{R}_{\text{SOFAR}}^*$, $\hat{R}_{\text{SOFAR}}^* := \arg \min_{R \in \mathcal{O}(m)} \|\hat{\Lambda}_{n, \text{SOFAR}} - \Lambda_n^* R\|_F^2$.

Table 3: Model selection and precision accuracy based on 200 replications, DGP (4.1), perfect simple structure with overlaps and sparse blocks (sparsity pattern (iii)) with respect to (n, p_n, m) .

| (p_n, m) | $n = 250$ | | | $n = 500$ | | | |
|------------|-----------|-----------------|-----------------|------------------|-----------------|-----------------|------------------|
| | SGF | SLSF | SOFAR | SGF | SLSF | SOFAR | |
| (60, 3) | C1 | 80.23 – 85.65 | 82.79 – 88.06 | 87.98 | 89.96 – 93.13 | 88.00 – 91.79 | 86.83 |
| | C2 | 100 – 100 | 100 – 100 | 92.33 | 100 – 100 | 100 – 100 | 94.20 |
| | MSE | 0.4210 – 0.4177 | 0.5458 – 0.5557 | 7.8310 (0.7397) | 0.2069 – 0.2056 | 0.2734 – 0.2756 | 6.4450 (0.3939) |
| (60, 4) | C1 | 80.83 – 86.61 | 81.79 – 87.47 | 85.93 | 90.53 – 93.68 | 87.01 – 91.14 | 85.81 |
| | C2 | 100 – 100 | 100 – 100 | 88.01 | 100 – 100 | 100 – 100 | 90.01 |
| | MSE | 0.5867 – 0.5828 | 0.8388 – 0.8504 | 18.39 (1.2519) | 0.2749 – 0.2731 | 0.3852 – 0.3916 | 15.7564 (0.6239) |
| (120, 3) | C1 | 79.48 – 85.03 | 83.17 – 88.46 | 89.00 | 90.01 – 93.27 | 88.41 – 92.23 | 89.16 |
| | C2 | 100 – 100 | 100 – 100 | 93.90 | 100 – 100 | 100 – 100 | 94.75 |
| | MSE | 0.8292 – 0.8196 | 1.0983 – 1.1078 | 11.8534 (1.4481) | 0.3654 – 0.3620 | 0.4825 – 0.4852 | 9.9180 (0.7379) |
| (120, 4) | C1 | 79.28 – 84.77 | 80.85 – 86.85 | 87.95 | 90.27 – 93.51 | 86.52 – 90.59 | 87.10 |
| | C2 | 100 – 100 | 99.99 – 99.98 | 89.67 | 100 – 100 | 100 – 100 | 91.07 |
| | MSE | 1.1254 – 1.1185 | 1.6724 – 2.0718 | 28.2858 (2.4809) | 0.5237 – 0.5198 | 0.7475 – 0.7565 | 27.0152 (1.2358) |
| (180, 3) | C1 | 78.59 – 84.07 | 82.81 – 88.17 | 90.16 | 89.80 – 93.19 | 89.25 – 92.77 | 89.78 |
| | C2 | 100 – 100 | 100 – 100 | 94.15 | 100 – 100 | 100 – 100 | 94.88 |
| | MSE | 1.2245 – 1.2107 | 1.6198 – 1.6406 | 16.3631 (2.1675) | 0.5678 – 0.5626 | 0.7420 – 0.7530 | 12.7403 (1.0939) |

Note: the column “SGF” refers to the estimator deduced from the Gaussian loss with SCAD and MCP penalization, respectively. The column “SLSF” refers to the estimator deduced from the least squares loss with SCAD and MCP penalization, respectively.

The MSE values for SOFAR in parenthesis are based on $\hat{\Lambda}_{n, \text{SOFAR}}^*$, with $\hat{\Lambda}_{n, \text{SOFAR}}^* := \Lambda_n^* \hat{R}_{\text{SOFAR}}^*$, $\hat{R}_{\text{SOFAR}}^* := \arg \min_{R \in \mathcal{O}(m)} \|\hat{\Lambda}_{n, \text{SOFAR}} - \Lambda_n^* R\|_F^2$.

Table 4: Model selection and precision accuracy based on 200 replications, DGP (4.1), arbitrary sparse structure and Ψ_n^* diagonal (sparsity pattern (iv)) with respect to (n, p_n, m) .

| (p_n, m) | | $n = 250$ | | | $n = 500$ | | |
|------------|-----|-----------------|-----------------|------------------|-----------------|-----------------|------------------|
| | | SGF | SLSF | SOFAR | SGF | SLSF | SOFAR |
| (60, 3) | C1 | 85.64 – 90.41 | 94.71 – 96.49 | 93.75 | 92.55 – 95.02 | 96.84 – 97.77 | 93.39 |
| | C2 | 100 – 100 | 100 – 99.96 | 92.98 | 99.98 – 99.98 | 99.98 – 99.98 | 95.43 |
| | MSE | 0.2291 – 0.2248 | 0.2498 – 0.2576 | 4.0267 (0.4398) | 0.1176 – 0.1162 | 0.1325 – 0.1347 | 2.7778 (0.2382) |
| (60, 4) | C1 | 86.82 – 91.19 | 94.45 – 96.43 | 93.02 | 93.04 – 95.61 | 96.57 – 97.55 | 92.53 |
| | C2 | 100 – 100 | 100 – 99.99 | 90.15 | 100 – 100 | 100 – 100 | 90.64 |
| | MSE | 0.3290 – 0.3232 | 0.3989 – 0.4080 | 7.2800 (0.7313) | 0.1505 – 0.1489 | 0.1837 – 0.1899 | 7.7528 (0.3875) |
| (120, 3) | C1 | 83.91 – 89.20 | 95.03 – 96.91 | 94.19 | 92.95 – 95.49 | 96.83 – 97.89 | 93.88 |
| | C2 | 100 – 100 | 100 – 100 | 94.09 | 100 – 100 | 100 – 100 | 95.44 |
| | MSE | 0.4946 – 0.4821 | 0.5103 – 0.5207 | 5.6643 (0.8235) | 0.1991 – 0.1960 | 0.2318 – 0.2366 | 5.3639 (0.4273) |
| (120, 4) | C1 | 83.66 – 88.90 | 94.65 – 96.81 | 93.59 | 92.89 – 95.51 | 96.88 – 97.89 | 92.74 |
| | C2 | 100 – 100 | 100 – 100 | 91.56 | 100 – 100 | 100 – 100 | 93.20 |
| | MSE | 0.6346 – 0.6179 | 0.7427 – 0.7609 | 11.9326 (1.4141) | 0.2787 – 0.2746 | 0.3481 – 0.3548 | 10.6349 (0.6905) |
| (180, 3) | C1 | 82.21 – 87.69 | 95.17 – 97.05 | 94.60 | 92.42 – 95.16 | 97.29 – 98.18 | 94.27 |
| | C2 | 100 – 100 | 100 – 100 | 94.37 | 100 – 100 | 100 – 100 | 95.52 |
| | MSE | 0.7393 – 0.7294 | 0.7443 – 0.7579 | 7.8451 (1.2388) | 0.3018 – 0.2970 | 0.3416 – 0.3478 | 6.3912 (0.6021) |

Note: the column “SGF” refers to the estimator deduced from the Gaussian loss with SCAD and MCP penalization, respectively. The column “SLSF” refers to the estimator deduced from the least squares loss with SCAD and MCP penalization, respectively.

The MSE values for SOFAR in parenthesis are based on $\hat{\Lambda}_{n, \text{SOFAR}}^*$, with $\hat{\Lambda}_{n, \text{SOFAR}}^* := \Lambda_n^* \hat{R}_{\text{SOFAR}}^*$, $\hat{R}_{\text{SOFAR}}^* := \arg \min_{R \in \mathcal{O}(m)} \|\hat{\Lambda}_{n, \text{SOFAR}} - \Lambda_n^* R\|_F^2$.

Table 5: Model selection and precision accuracy based on 200 replications, DGP (4.1), arbitrary sparse structure and Ψ_n^* non-diagonal (sparsity pattern (v)) with respect to (n, p_n, m) .

| (p_n, m) | $n = 250$ | | | $n = 500$ | | | |
|------------|-----------|-----------------|-----------------|------------------|-----------------|-----------------|------------------|
| | SGF | SLSF | SOFAR | SGF | SLSF | SOFAR | |
| (60, 3) | C1 | 84.66 – 89.67 | 94.46 – 96.35 | 93.93 | 89.61 – 93.31 | 96.14 – 97.35 | 93.54 |
| | C2 | 100 – 100 | 99.98 – 99.98 | 92.91 | 100 – 100 | 100 – 100 | 94.44 |
| | MSE | 0.2592 – 0.2544 | 0.2644 – 0.2713 | 3.7779 (0.4345) | 0.1165 – 0.1138 | 0.1284 – 0.1297 | 3.0521 (0.2431) |
| (60, 4) | C1 | 84.36 – 89.64 | 94.11 – 96.16 | 92.58 | 90.56 – 93.48 | 96.63 – 97.67 | 92.46 |
| | C2 | 100 – 100 | 99.94 – 99.93 | 91.39 | 100 – 100 | 100 – 100 | 92.35 |
| | MSE | 0.3534 – 0.3485 | 0.4075 – 0.4206 | 7.4735 (0.7177) | 0.1552 – 0.1527 | 0.1790 – 0.1846 | 6.5640 (0.3788) |
| (120, 3) | C1 | 83.25 – 88.47 | 94.93 – 96.72 | 94.18 | 92.19 – 94.83 | 96.76 – 97.74 | 93.62 |
| | C2 | 100 – 100 | 100 – 100 | 93.27 | 100 – 100 | 100 – 100 | 94.78 |
| | MSE | 0.4862 – 0.4782 | 0.4760 – 0.4920 | 6.9414 (0.8543) | 0.1981 – 0.1947 | 0.2363 – 0.2413 | 5.3025 (0.4199) |
| (120, 4) | C1 | 83.69 – 88.99 | 95.01 – 96.89 | 93.85 | 92.34 – 95.24 | 96.79 – 97.86 | 93.42 |
| | C2 | 100 – 100 | 100 – 100 | 89.72 | 100 – 100 | 100 – 100 | 92.81 |
| | MSE | 0.6373 – 0.6264 | 0.7082 – 0.7272 | 13.5563 (1.3894) | 0.2805 – 0.2758 | 0.3499 – 0.3582 | 10.6029 (0.7078) |
| (180, 3) | C1 | 82.01 – 87.43 | 95.43 – 97.16 | 94.75 | 92.31 – 94.95 | 96.90 – 97.94 | 94.01 |
| | C2 | 100 – 100 | 100 – 100 | 93.69 | 100 – 100 | 100 – 100 | 95.68 |
| | MSE | 0.7208 – 0.7178 | 0.7267 – 0.7481 | 8.2446 (1.1955) | 0.3034 – 0.2977 | 0.3569 – 0.3624 | 6.3573 (0.6182) |

Note: the column “SGF” refers to the estimator deduced from the Gaussian loss with SCAD and MCP penalization, respectively. The column “SLSF” refers to the estimator deduced from the least squares loss with SCAD and MCP penalization, respectively.

The MSE values for SOFAR in parenthesis are based on $\hat{\Lambda}_{n, \text{SOFAR}}^*$, with $\hat{\Lambda}_{n, \text{SOFAR}}^* := \Lambda_n^* \hat{R}_{\text{SOFAR}}^*$, $\hat{R}_{\text{SOFAR}}^* := \arg \min_{R \in \mathcal{O}(m)} \|\hat{\Lambda}_{n, \text{SOFAR}} - \Lambda_n^* R\|_F^2$.

Table 6: Model selection and precision accuracy based on 200 replications, DGP (4.2), arbitrary sparse structure and Ψ_n^* non-diagonal (sparsity pattern (v)) with respect to (n, p_n, m) .

| (p_n, m) | $n = 250$ | | | $n = 500$ | | | |
|------------|-----------|-----------------|-----------------|------------------|-----------------|-----------------|------------------|
| | SGF | SLSF | SOFAR | SGF | SLSF | SOFAR | |
| (60, 3) | C1 | 84.90 – 89.61 | 91.40 – 93.87 | 93.36 | 87.41 – 90.87 | 88.96 – 90.73 | 93.26 |
| | C2 | 100 – 100 | 98.98 – 98.93 | 92.37 | 100 – 100 | 99.78 – 99.76 | 94.83 |
| | MSE | 0.5828 – 0.5859 | 1.1727 – 1.0879 | 4.3293 (0.7238) | 0.2445 – 0.2564 | 0.4521 – 0.4369 | 3.6107 (0.4049) |
| (60, 4) | C1 | 84.80 – 89.59 | 89.75 – 92.11 | 92.83 | 90.25 – 93.18 | 90.20 – 92.35 | 91.88 |
| | C2 | 100 – 100 | 99.14 – 98.82 | 89.43 | 100 – 100 | 99.54 – 99.37 | 92.82 |
| | MSE | 0.8089 – 0.8162 | 1.3863 – 1.4845 | 8.7268 (1.2287) | 0.3473 – 0.3494 | 0.8278 – 0.9286 | 7.0553 (0.6235) |
| (120, 3) | C1 | 84.07 – 89.52 | 90.48 – 93.10 | 94.36 | 92.17 – 94.74 | 91.20 – 93.21 | 93.62 |
| | C2 | 100 – 100 | 99.88 – 99.69 | 92.77 | 100 – 100 | 99.83 – 99.84 | 95.23 |
| | MSE | 1.2823 – 1.3134 | 1.6126 – 1.7297 | 7.9089 (1.4714) | 0.5463 – 0.5665 | 1.0274 – 1.0343 | 5.8175 (0.7627) |
| (120, 4) | C1 | 83.58 – 89.12 | 90.85 – 93.45 | 93.61 | 92.84 – 95.53 | 93.07 – 94.81 | 92.78 |
| | C2 | 100 – 100 | 99.79 – 99.55 | 90.65 | 100 – 100 | 99.88 – 99.81 | 91.97 |
| | MSE | 1.5176 – 1.5428 | 2.2719 – 2.3588 | 13.4791 (2.4224) | 0.5598 – 0.5742 | 1.0539 – 1.1916 | 12.8153 (1.2390) |
| (180, 3) | C1 | 82.39 – 87.79 | 91.58 – 93.82 | 94.62 | 91.85 – 94.84 | 92.46 – 94.31 | 94.00 |
| | C2 | 100 – 100 | 99.79 – 99.51 | 93.61 | 100 – 100 | 99.91 – 99.86 | 94.61 |
| | MSE | 1.8582 – 1.9028 | 2.3531 – 2.4386 | 9.8763 (2.2220) | 0.8276 – 0.8543 | 1.1838 – 1.1708 | 8.0994 (1.1578) |

Note: the column “SGF” refers to the estimator deduced from the Gaussian loss with SCAD and MCP penalization, respectively. The column “SLSF” refers to the estimator deduced from the least squares loss with SCAD and MCP penalization, respectively.

The MSE values for SOFAR in parenthesis are based on $\hat{\Lambda}_{n, \text{SOFAR}}^*$, with $\hat{\Lambda}_{n, \text{SOFAR}}^* := \Lambda_n^* \hat{R}_{\text{SOFAR}}^*$, $\hat{R}_{\text{SOFAR}}^* := \arg \min_{R \in \mathcal{O}(m)} \|\hat{\Lambda}_{n, \text{SOFAR}} - \Lambda_n^* R\|_F^2$.

5 Real data applications

5.1 Portfolio allocation

In this section, we assess the variance-covariance forecast performances of multiple models using financial data, where we rank the forecast accuracy by the model confidence set (MCS) of Hansen et al. (2011), which provides a testing framework for the null hypothesis of forecast equivalence across subsets of models. We first start with a description of the data. Hereafter, we do not index by n the model parameters and p to ease the notations.

5.1.1 Data

We consider hereafter the stochastic process $(r_t)_{t \in \mathbb{Z}}$ in \mathbb{R}^p of the log-stock returns, where $r_{t,j} = 100 \times \log(P_{t,j}/P_{t-1,j})$, $1 \leq j \leq p$ with $P_{t,j}$ the stock price of the j -th index at time t . We study three financial portfolios: a low-dimensional portfolio of daily log-returns composed with the MSCI stock index based on the sample December 1998-March 2018, which yields a sample size $n = 5006$, and for $p = 23$ countries (Australia, Austria, Belgium, Canada, Denmark, Finland, France, Germany, Greece, Hong Kong, Ireland, Italy, Japan, Netherlands, New Zealand, Norway, Portugal, Singapore, Spain, Sweden, Switzerland, the United-Kingdom, the United-States); a mid-dimensional portfolio of daily log-returns based on the S&P 100, consisting of firms that have been continuously included in the index over the period February 2010 – January 2020, excluding AbbVie Inc., Dow Inc., General Motors, Kraft Heinz, Kinder Morgan and PayPal Holdings, which leaves $p = 94$ with a sample size $n = 2500$; a high-dimensional portfolio of daily log-returns based on the S&P 500, consisting of the firms that have been continuously included in the index over the period September 2014 – January 2022, excluding Etsy Inc., SolarEdge Technologies Inc., PayPal, Hewlett Packard Enterprise, Under Armour (class C), Fortive, Lamb Weston, Ingersoll Rand Inc., Ceridian HCM, Linde PLC, Moderna, Fox Corporation (class A and B), Dow Inc., Corteva Inc., Amcor, Otis Worldwide, Carrier Global, Match Group, Viatrix Inc., which leaves $p = 480$ assets with a sample size $n = 1901$. Hereafter, the portfolios are denoted by MSCI, S&P 100 and S&P 500, respectively¹.

¹The MSCI, S&P 100 and S&P 500 data can be found on <https://www.msci.com/>, <https://finance.yahoo.com> and <https://macrobond.com>, respectively.

5.1.2 Global Minimum Variance Portfolio (GMVP)

The economic performances are assessed through the GMVP investment strategy. The latter problem at time t , in the absence of short-sales constraints, is defined as

$$\min_{w_t} w_t^\top \widehat{\Sigma}_t w_t, \quad \text{s.t. } \iota^\top w_t = 1, \quad (5.1)$$

where $\widehat{\Sigma}_t$ is the predicted $p \times p$ variance-covariance matrix and ι is a $p \times 1$ vector of 1's. The explicit solution is given by $\omega_t = \widehat{\Sigma}_t^{-1} \iota / \iota^\top \widehat{\Sigma}_t^{-1} \iota$: as a function depending only on $\widehat{\Sigma}_t$, the GMVP performance essentially depends on the precise measurement of the variance-covariance matrix. The following out-of-sample performance metrics (annualized) will be reported: **AVG** as the average of the out-of-sample portfolio returns, multiplied by 252; **SD** as the standard deviation of the out-of-sample portfolio returns, multiplied by $\sqrt{252}$; **IR** as the information ratio computed as **AVG/SD**. The key performance measure is the out-of-sample **SD**. The GMVP problem essentially aims to minimize the variance rather than to maximize the expected return. Hence, as emphasized in [Engle et al. \(2019\)](#), Section 6.2, high **AVG** and **IR** are desirable but should be considered of secondary importance compared with the quality of the measure of a variance-covariance matrix estimator.

5.1.3 Competing variance-covariance matrix estimators

We will rank the following models according to the MCS procedure, where, excluding the DCC, the competing models provide fixed estimators of Σ_t , i.e., $\widehat{\Sigma}_t = \widehat{\Sigma}$:

- **Sample-VC**: the sample estimator of the variance-covariance.
- **covM1**: the predicted $\widehat{\Sigma}$ shrunk towards a one-factor market model, where the factor is defined as the cross-sectional average of all the components of r_t . The idiosyncratic volatility of the residuals allows the target to preserve the diagonal of the sample covariance matrix. This estimator was developed by [Ledoit and Wolf \(2003\)](#).
- **GIS**: the geometric-inverse shrinkage estimator $\widehat{\Sigma}$, which is a nonlinear shrinkage estimator based on the symmetrized Kullback-Leibler loss: this static estimator can be considered as geometrically averaging the linear-inverse shrinkage (LIS) estimator with the quadratic-inverse shrinkage (QIS) estimator of [Ledoit and Wolf \(2022\)](#).
- **SAF**: the factor model $\widehat{\Sigma} = \widehat{\Lambda} \widehat{\Lambda}^\top + \widehat{\Psi}$, where Ψ is non-diagonal but sparse with bounded eigenvalues. This is the sparse approximate factor (SAF) model of [Bai and](#)

Li (2016) estimated by adaptive LASSO Gaussian QML under $\Lambda^\top \Psi^{-1} \Lambda$ diagonal. More details on the SAF and implementation are provided in Subsection E.2 of the Appendix.

- **SGF**: the factor model $\hat{\Sigma} = \hat{\Lambda} \hat{\Lambda}^\top + \hat{\Psi}$, estimated by criterion (2.1) with the Gaussian loss for a general arbitrary sparse Λ , Ψ diagonal, with SCAD (SGF^{scad}) and MCP (SGF^{mcp}).
- **SLSF**: the factor model $\hat{\Sigma} = \hat{\Lambda} \hat{\Lambda}^\top + \hat{\Psi}$, estimated by criterion (2.1) with the least squares loss for a general arbitrary sparse Λ , Ψ diagonal with SCAD (SLSF^{scad}) and MCP (SLSF^{mcp}).
- **DCC**: the scalar DCC of Engle (2002) with GARCH(1,1) dynamics for the marginals. This is a dynamic estimator of Σ_t : once the model is estimated in-sample, the estimated parameters are plugged in the out-of-sample period to generate the out-of-sample sequence of Σ_t , providing a sequence of GMVP weights. The estimation is carried out by a standard two-step Gaussian QML. More details on the DCC and estimation, in particular the composite likelihood method, are provided in Subsection E.1 of the Appendix.

It is worthwhile to include variance-covariance models that are not derived from a factor model, thereby motivating the inclusion of the scalar DCC in the analysis.

As in Section 4, we set $a_{\text{scad}} = 3.7$, $b_{\text{mcp}} = 3.5$. The selection of an optimal γ_n is based on the out-of-sample cross-validation procedure detailed in Subsection D.2 of the Appendix. As emphasized in De Nard et al. (2021), there is no consensual selection procedure of the number of factors so that it is of interest to assess the sensitivity of the factor-model-based allocation performances with respect to m : we set $m \in \{1, 2, 3, 4, 5\}$. It is worth noting that the SOFAR procedure estimates a sparse loading matrix only and does not allow to obtain an estimator of the variance-covariance matrix: the SOFAR procedure is thus not under consideration. The economic performances are ranked out-of-sample by the MCS test, which takes the distance based on the difference of the squared returns of portfolios i and j , defined as $u_{ij,t} = (\mu_{i,t} - \bar{\mu}_i)^2 - (\mu_{j,t} - \bar{\mu}_j)^2$, with $\mu_{k,t} = w_{k,t}^\top y_t$ the portfolio return at time t , where $w_{k,t}$ represents the GMVP weight deduced from variance-covariance model k , and $\bar{\mu}_k$ is the average portfolio return over the period. The MCS test is evaluated at the 10% level based on the range statistic and with block bootstrap with 10,000 replications: see Hansen et al. (2003) for further technical procedures. We report below the out-of-sample periods used for the test accuracy and the number of factors \hat{m}

selected in-sample by the eigenvalue-based procedure of [Onatski \(2010\)](#) on an indicative basis:

- MSCI portfolio: in sample is 01/01/1999 – 07/01/2010 with $\hat{m} = 1$ and out-of-sample is 07/02/2010 – 03/12/2018.
- S&P 100 portfolio: in sample is 02/19/2010 – 04/22/2014 with $\hat{m} = 3$ and out-of-sample is 04/23/2014 – 01/23/2020.
- S&P 500 portfolio: in sample is 09/25/2014 – 12/12/2018 with $\hat{m} = 1$ and out-of-sample is 12/13/2018 – 01/27/2022.

The GMVP performance results are displayed in [Table 7](#), and they can be summarized as follows - unless stated otherwise, the results are with respect to **SD** -: the sparse factor loading-based strategy enters the MCS in the low, mid and high-dimensional cases; the DCC provides the best performance for the low-dimensional portfolio only; for the mid-dimensional portfolio, the least squares-based SLSF estimator with $m = 4, 5$ only enters the MCS; in the high-dimensional portfolio, although the SAF seems more appropriate to measure the variance-covariance suggesting the existence of cross-correlation in ϵ_t , the sparse factor loading SGF for $m = 2, 3$ still enters the MCS at 10%-level.

Table 7: Annualized GMVP performance metrics for various estimators.

| | MSCI | | | | S&P 100 | | | | S&P 500 | | | |
|-----------------------------------|-------------------------|--------------|-------|--------------|-------------------------|---------------|-------|--------------|-------------------------|---------------|-------|--------------|
| | 07/02/2010 - 03/12/2018 | | | | 04/23/2014 - 01/23/2020 | | | | 12/13/2018 - 01/27/2022 | | | |
| | AVG | SD | IR | MCS | AVG | SD | IR | MCS | AVG | SD | IR | MCS |
| DCC | 7.482 | 9.551 | 0.783 | 1.000 | 17.293 | 11.941 | 1.448 | 0 | 15.278 | 20.146 | 0.758 | 0.024 |
| Sample-VC | 9.014 | 10.003 | 0.901 | 0 | 13.187 | 11.412 | 1.156 | 0 | 2.808 | 22.090 | 0.127 | 0.007 |
| SGF ₁ ^{scad} | 7.629 | 11.172 | 0.683 | 0 | 9.426 | 12.617 | 0.747 | 0 | 4.288 | 21.472 | 0.200 | 0.002 |
| SGF ₁ ^{mcp} | 7.629 | 11.172 | 0.683 | 0 | 9.469 | 12.767 | 0.742 | 0 | 4.219 | 21.532 | 0.196 | 0.002 |
| SGF ₂ ^{scad} | 8.980 | 9.625 | 0.933 | 0.832 | 11.405 | 13.309 | 0.857 | 0 | 7.904 | 17.833 | 0.443 | 0.231 |
| SGF ₂ ^{mcp} | 8.978 | 9.625 | 0.933 | 0.832 | 11.555 | 13.265 | 0.871 | 0 | 7.914 | 17.883 | 0.443 | 0.024 |
| SGF ₃ ^{scad} | 7.891 | 9.955 | 0.793 | 0 | 15.702 | 12.403 | 1.266 | 0 | 7.124 | 17.602 | 0.405 | 0.798 |
| SGF ₃ ^{mcp} | 8.397 | 9.780 | 0.859 | 0 | 16.035 | 12.456 | 1.287 | 0 | 7.221 | 17.670 | 0.409 | 0.725 |
| SGF ₄ ^{scad} | 7.866 | 9.985 | 0.788 | 0 | 14.070 | 12.419 | 1.133 | 0 | 8.427 | 19.041 | 0.443 | 0.024 |
| SGF ₄ ^{mcp} | 8.511 | 9.809 | 0.868 | 0 | 14.774 | 12.338 | 1.197 | 0 | 7.682 | 18.745 | 0.410 | 0.024 |
| SGF ₅ ^{scad} | 9.281 | 9.977 | 0.930 | 0 | 11.373 | 12.001 | 0.948 | 0 | 8.748 | 19.438 | 0.450 | 0.024 |
| SGF ₅ ^{mcp} | 9.192 | 9.989 | 0.920 | 0 | 12.029 | 11.907 | 1.010 | 0 | 8.162 | 19.162 | 0.426 | 0.024 |
| SLSF ₁ ^{scad} | 7.961 | 10.889 | 0.731 | 0 | 9.069 | 12.583 | 0.721 | 0 | 4.411 | 21.430 | 0.206 | 0.007 |
| SLSF ₁ ^{mcp} | 7.961 | 10.889 | 0.731 | 0 | 9.091 | 12.774 | 0.712 | 0 | 4.315 | 21.513 | 0.201 | 0.002 |
| SLSF ₂ ^{scad} | 8.552 | 9.730 | 0.879 | 0.002 | 9.017 | 11.823 | 0.763 | 0 | 3.677 | 21.346 | 0.172 | 0.007 |
| SLSF ₂ ^{mcp} | 9.021 | 9.655 | 0.934 | 0.018 | 9.025 | 12.041 | 0.750 | 0 | 3.645 | 21.387 | 0.170 | 0.007 |
| SLSF ₃ ^{scad} | 8.829 | 9.784 | 0.902 | 0.002 | 8.841 | 11.331 | 0.780 | 0 | 5.384 | 19.566 | 0.275 | 0.007 |
| SLSF ₃ ^{mcp} | 8.858 | 9.723 | 0.911 | 0.017 | 8.882 | 11.454 | 0.776 | 0 | 5.881 | 19.300 | 0.305 | 0.007 |
| SLSF ₄ ^{scad} | 8.715 | 9.963 | 0.875 | 0 | 8.508 | 10.941 | 0.778 | 0.951 | 4.275 | 19.195 | 0.223 | 0.007 |
| SLSF ₄ ^{mcp} | 8.826 | 9.948 | 0.887 | 0 | 8.656 | 11.002 | 0.787 | 0.040 | 4.425 | 19.407 | 0.228 | 0.007 |
| SLSF ₅ ^{scad} | 9.025 | 9.820 | 0.919 | 0 | 8.000 | 11.629 | 0.688 | 0 | 5.162 | 19.741 | 0.262 | 0.007 |
| SLSF ₅ ^{mcp} | 9.028 | 10.007 | 0.902 | 0 | 8.190 | 10.934 | 0.749 | 1.000 | 5.001 | 19.882 | 0.252 | 0.007 |
| SAF ₁ | 8.063 | 10.446 | 0.772 | 0 | 11.031 | 12.137 | 0.909 | 0 | 3.660 | 22.041 | 0.166 | 0.002 |
| SAF ₂ | 8.856 | 9.769 | 0.907 | 0 | 10.927 | 11.786 | 0.927 | 0 | 7.690 | 18.500 | 0.416 | 0.024 |
| SAF ₃ | 8.837 | 9.902 | 0.893 | 0 | 14.595 | 11.815 | 1.235 | 0 | 8.014 | 25.121 | 0.319 | 0.007 |
| SAF ₄ | 8.679 | 9.939 | 0.873 | 0 | 14.412 | 11.759 | 1.226 | 0 | 12.330 | 19.223 | 0.641 | 0.007 |
| SAF ₅ | 8.898 | 10.099 | 0.881 | 0 | 14.100 | 11.606 | 1.215 | 0 | 6.359 | 17.456 | 0.364 | 1.000 |
| GIS | 9.004 | 9.995 | 0.901 | 0 | 13.073 | 11.285 | 1.158 | 0.040 | 5.820 | 19.849 | 0.293 | 0.007 |
| covMI ₁ | 8.975 | 9.988 | 0.899 | 0 | 12.741 | 11.370 | 1.121 | 0.001 | 4.125 | 20.103 | 0.205 | 0.007 |

Note: The lowest **SD** figure is in bold face. The index k in $\text{SGF}_k^{\text{pen}}$, $\text{SLSF}_k^{\text{pen}}$ and SAF_k represents the number of factors. The out-of-sample periods are indicated above **AVG**, **SD**, **IR** and **MCS**. The out-of-sample dates are reported below the portfolio name.

5.2 Diffusion index data

We now propose to investigate how the estimation of the factors impact the prediction accuracy. To do so, we follow the experiment of [Bai and Liao \(2016\)](#), Section 5.3., which concerns the industrial production based on macroeconomic time series of the United

States. It consists of a macroeconomic panel of $p = 131$ series from 1959 to 2007, representing a sample of size $\mathcal{T} = 528$. In the same spirit as in [Stock and Watson \(2002\)](#) and [Bai and Liao \(2016\)](#), we denote by Y_t the scalar time series variable to be predicted and by X_t the p -dimensional vector of candidate predictors, and assume that (X_t, Y_t) satisfies a factor model decomposition with m common latent factors F_t :

$$Y_{t+h}^h = \alpha_h + \beta_h F_t + \gamma_h W_{t,l} + u_{t+h}, \quad X_t = \Lambda F_t + \epsilon_t,$$

where h is the forecast horizon, $Y_{t+h}^h = h^{-1} \sum_{i=1}^h Y_{t+i}$ is the h -step-ahead variable to be predicted and defined as the industrial production, $W_{t,l} = (Y_t, \dots, Y_{t-l})^\top \in \mathbb{R}^l$ contains the lagged values of Y_t , and u_{t+h} is the forecast error. We construct the forecasts of Y_{t+h}^h according to a fixed rolling window of size $n = 422$ (that is $0.8\mathcal{T}$), where for each window we estimate the factor model of X_t and estimate the latent factors F_t . Finally, we compute the forecast of Y_{n+h}^h as $\hat{Y}_{n+h}^h = \hat{\alpha}_h + \hat{\beta}_h \hat{F}_n + \hat{\gamma}_h W_{n,l}$, where $\hat{\alpha}_h, \hat{\beta}_h, \hat{\gamma}_h$ are obtained by regressing Y_{t+h}^h on $\hat{F}_t, W_{t,l}$ with intercept. The squared prediction error is defined as $(Y_{n+h}^h - \hat{Y}_{n+h}^h)^2$. All the data are standardized.

The following methods are employed to obtain \hat{F}_t : PCA, SOFAR, SAF, SGF, SLSF. The estimator deduced from PCA follows from [Bai \(2003\)](#), that is the estimator of the factors $\hat{\mathbf{F}} \in \mathbb{R}^{n \times m}$ with t -th row \hat{F}_t^\top is \sqrt{n} times eigenvectors corresponding to the m largest eigenvalues of $\mathbf{X}\mathbf{X}^\top \in \mathbb{R}^{n \times n}$, and $\hat{\Lambda} = \mathbf{X}^\top \hat{\mathbf{F}}/n$. As for SAF, SGF, SLSF, \hat{F}_t is obtained by the GLS estimator. Regarding SOFAR, its optimal regularization parameter was selected as the one that achieves the best performance in the simulation experiments. However, in the case of real data, the selection of the optimal tuning parameter that ensures the best out-of-sample performance is unfeasible. Therefore, from the candidate values $(e^{-2}, e^{-2.25}, \dots, e^{+5})$, the regularization parameters are determined using BIC, as recommended by the authors. The out-of-sample prediction performances are assessed through the mean squared out-of-sample forecasting error (MSE) relative to the PCA method for $h = 12, 24$, $l = 1, 3$ and $m = 5, 6, 7$. The choice for m follows from the setting of [Bai and Liao \(2016\)](#), who considered $m = 7, 8$: we preferred to consider a slightly lower number of factors for parsimony. The mean squared MSE is defined as $s^{-1} \sum_{r=0}^{s-1} (Y_{r+n+h}^h - \hat{Y}_{r+n+h}^h)^2$, with $s = \mathcal{T} - n - h$. [Table 8](#) reports the MSE metrics relative to the PCA method. It is observed that our proposed method outperforms SOFAR, excluding $h = 12, l = 3, m = 6$ only. We notice SAF has the best performances for $m = 5$, but when $m = 6, 7$, the sparse factor model is beneficial for prediction. We also observe that in both period-ahead forecasts h , $m = 5$ is much better than $m = 6, 8$, for SAF, SGF and SLSF.

Table 8: Relative MSE for out-of-sample predictions.

| (h, l, m) | SOFAR | SAF | SGF ^{scad} | SGF ^{mcp} | SLSF ^{scad} | SLSF ^{mcp} |
|----------------------|--------|--------|---------------------|--------------------|----------------------|---------------------|
| $m = 5$ | 0.9267 | 0.7057 | 0.7317 | 0.7881 | 0.8799 | 0.8537 |
| $(12, 1, m)$ $m = 6$ | 0.8811 | 0.9564 | 0.9448 | 0.9417 | 0.9191 | 0.8758 |
| $m = 7$ | 0.9224 | 1.0733 | 0.7985 | 0.8961 | 1.0090 | 1.0173 |
| $m = 5$ | 0.9304 | 0.7136 | 0.7509 | 0.7979 | 0.9024 | 0.8734 |
| $(12, 3, m)$ $m = 6$ | 0.8690 | 0.9588 | 0.9432 | 0.9453 | 0.9214 | 0.8787 |
| $m = 7$ | 0.9176 | 1.0826 | 0.8106 | 0.9116 | 1.0254 | 1.0309 |
| $m = 5$ | 0.9257 | 0.6987 | 0.7629 | 0.7385 | 0.7699 | 0.7695 |
| $(24, 1, m)$ $m = 6$ | 0.9544 | 0.8958 | 0.8130 | 0.8510 | 0.7857 | 0.7919 |
| $m = 7$ | 0.9230 | 0.8671 | 0.8672 | 0.8144 | 0.9118 | 0.9179 |
| $m = 5$ | 0.9296 | 0.7051 | 0.7658 | 0.7484 | 0.7853 | 0.7841 |
| $(24, 3, m)$ $m = 6$ | 0.9542 | 0.8973 | 0.8172 | 0.8700 | 0.7901 | 0.7977 |
| $m = 7$ | 0.9252 | 0.8599 | 0.8630 | 0.8103 | 0.9191 | 0.9305 |

6 Discussion and conclusion

We study the asymptotic properties of sparse factor models. We establish the sparsistency property of the corresponding penalized M-estimator, where the identification condition allows for a broad range of sparsity patterns.

Throughout the paper, we worked under a diagonal variance-covariance of the idiosyncratic error variables. An interesting direction would consist in replacing this condition by a non-diagonal but sparse variance-covariance matrix within the sparse factor loading framework. This would raise issues regarding the conditions for identification to disentangle the sparsity patterns of Λ_n and Ψ_n . We shall leave it for the future research.

Acknowledgments

This work was supported by JSPS KAKENHI Grant (JP22K13377 to BP; JP20K19756 and JP20H00601 to YT). The authors warmly thank Jan Magnus for his suggestions.

References

- T. Anderson. *An Introduction to Multivariate Statistical Analysis*. Wiley Series in Probability and Statistics. Wiley, 2003.
- T. Anderson and Y. Amemiya. The asymptotic normal distribution of estimators in factor analysis under general conditions. *The Annals of Statistics*, 16(2):759–771, 1988. [10.1214/aos/1176350834](https://doi.org/10.1214/aos/1176350834).
- T. Anderson and H. Rubin. Statistical inference in factor analysis. *Proceedings of the Third Berkeley Symposium on Mathematical Statistics and Probability*, V:111–150, 1956.
- J. Bai. Inferential theory for factor models of large dimensions. *Econometrica*, 71(1):135–171, 2003. [10.1111/1468-0262.00392](https://doi.org/10.1111/1468-0262.00392).
- J. Bai and K. Li. Statistical analysis of factor models of high dimension. *The Annals of Statistics*, 40(1):436–465, 2012. [10.1214/11-AOS966](https://doi.org/10.1214/11-AOS966).
- J. Bai and K. Li. Maximum likelihood estimation and inference for approximate factor models of high dimension. *The Review of Economics and Statistics*, 98(2):298–309, 2016. [10.1162/REST_a_00519](https://doi.org/10.1162/REST_a_00519).
- J. Bai and K. Liao. Efficient estimation of approximate factor models via penalized maximum likelihood. *Journal of Econometrics*, 191(1):1–18, 2016. [10.1016/j.jeconom.2015.10.003](https://doi.org/10.1016/j.jeconom.2015.10.003).
- J. Bai and S. Ng. Approximate factor models with weaker loadings. *Journal of Econometrics*, 235(2):1893–1916, 2023. [10.1016/j.jeconom.2023.01.027](https://doi.org/10.1016/j.jeconom.2023.01.027).
- V. Cerqueira, L. Torgo, and I. Mozetic. Evaluating time series forecasting models: An empirical study on performance estimation methods. *Machine Learning*, 109:1997–2028, 2020. [10.1007/s10994-020-05910-7](https://doi.org/10.1007/s10994-020-05910-7).
- G. Chamberlain and M. Rothschild. Arbitrage, factor structure and mean–variance analysis in large asset markets. *Econometrica*, 51(5):1305–1324, 1983. [10.2307/1912275](https://doi.org/10.2307/1912275).
- M. Daniele, W. Pohlmeier, and A. Zagidullina. A sparse approximate factor model for high-dimensional covariance matrix estimation and portfolio selection. *Journal of Financial Econometrics*,, pages 1–30, 2024. [10.1093/jjfinec/nbae017](https://doi.org/10.1093/jjfinec/nbae017).

- G. De Nard, O. Ledoit, and M. Wolf. Factor models for portfolio selection in large dimensions: The good, the better and the ugly. *Journal of Financial Econometrics*, 19(2):236–257, 2021. [10.1093/jjfines/nby033](https://doi.org/10.1093/jjfines/nby033).
- R. Engle. Dynamic Conditional Correlation: A simple class of multivariate generalized autoregressive conditional heteroskedasticity models. *Journal of Business & Economic Statistics*, 20(3):339–350, 2002. [10.1198/073500102288618487](https://doi.org/10.1198/073500102288618487).
- R. Engle, O. Ledoit, and M. Wolf. Large dynamic covariance matrices. *Journal of Business & Economic Statistics*, 37(2):363–375, 2019. [10.1080/07350015.2017.1345683](https://doi.org/10.1080/07350015.2017.1345683).
- J. Fan and R. Li. Variable selection via nonconcave penalized likelihood and its oracle properties. *Journal of the American statistical Association*, 96(456):1348–1360, 2001. [10.1198/016214501753382273](https://doi.org/10.1198/016214501753382273).
- J. Fan and H. Peng. Nonconcave penalized likelihood with a diverging number of parameters. *The Annals of Statistics*, 32(3):928–961, 2004. [10.1214/009053604000000256](https://doi.org/10.1214/009053604000000256).
- J. Fan, Y. Liao, and M. Mincheva. High-dimensional covariance matrix estimation in approximate factor models. *The Annals of Statistics*, 39(6):3320–3356, 2011. [10.1214/11-AOS944](https://doi.org/10.1214/11-AOS944).
- J. Fermanian and B. Pognard. Sparse M-estimators in semi-parametric copula models. *Bernoulli*, 30(3):2475–2500, 2024. [10.3150/23-BEJ1681](https://doi.org/10.3150/23-BEJ1681).
- S. Freyaldenhoven. Identification through sparsity in factor models. *Federal Reserve Bank of Philadelphia Working Paper 20-25/R*, 2023. URL https://simonfreyaldenhoven.github.io/papers/factor_rotation.pdf.
- P. Hansen, A. Lunde, and M. Nason. Choosing the best volatility models: The model confidence set approach. *Oxford Bulletin of Economics and Statistics*, 65(s1):839–861, 2003. [10.1046/j.0305-9049.2003.00086.x](https://doi.org/10.1046/j.0305-9049.2003.00086.x).
- P. Hansen, A. Lunde, and M. Nason. The model confidence set. *Econometrica*, 79(2):453–497, 2011. [10.3982/ECTA5771](https://doi.org/10.3982/ECTA5771).
- T. Hastie, R. Tibshirani, and J. Friedman. *The Elements of Statistical Learning: Data mining, inference, and prediction*. Springer Series in Statistics. Springer, New York, 2nd edition, 2009. [10.1007/978-0-387-84858-7](https://doi.org/10.1007/978-0-387-84858-7).
- K. Hirose and Y. Terada. Sparse and simple structure estimation via prenet penalization. *Psychometrika*, 88(4):1381–1406, 2023. [10.1007/s11336-022-09868-4](https://doi.org/10.1007/s11336-022-09868-4).

- Y. Kano. Consistency of estimators in factor analysis. *Journal of the Japan Statistical Society*, 13(2):137–144, 1983. [10.11329/jjss1970.13.137](https://doi.org/10.11329/jjss1970.13.137).
- C. Lam and J. Fan. Sparsistency and rates of convergence in large covariance matrix estimation. *The Annals of Statistics*, 37(6B):4254–4278, 2009. [10.1214/09-AOS720](https://doi.org/10.1214/09-AOS720).
- O. Ledoit and M. Wolf. Improved estimation of the covariance matrix of stock returns with an application to portfolio selection. *Journal of Empirical Finance*, 10(5):603–621, 2003. [10.1016/S0927-5398\(03\)00007-0](https://doi.org/10.1016/S0927-5398(03)00007-0).
- O. Ledoit and M. Wolf. Quadratic shrinkage for large covariance matrices. *Bernoulli*, 28(3):1519–1547, 2022. [10.3150/20-BEJ1315](https://doi.org/10.3150/20-BEJ1315).
- P. Loh and M. Wainwright. Regularized M-estimators with non-convexity: Statistical and algorithmic theory for local optima. *Journal of Machine Learning Research*, 16:559–616, 2015. URL <https://www.jmlr.org/papers/v16/loh15a.html>.
- J. Magnus and H. Neudecker. *Matrix Differential Calculus with Applications in Statistics and Econometrics*. Wiley Series in Probability and Statistics. John Wiley & Sons Ltd, 3rd edition, 2019. [10.1002/9781119541219](https://doi.org/10.1002/9781119541219).
- I. Ohn, L. Lin, and Y. Kim. A bayesian sparse factor model with adaptive posterior concentration. *Bayesian Analysis*, 19(4):1277–1301, 2024. [10.1214/23-BA1392](https://doi.org/10.1214/23-BA1392).
- A. Onatski. Determining the number of factors from empirical distribution of eigenvalues. *The Review of Economics and Statistics*, 92(4):1004–1016, 2010. [10.1162/REST_a.00043](https://doi.org/10.1162/REST_a.00043).
- C. Pakel, N. Shephard, K. Sheppard, and R. Engle. Fitting vast dimensional time-varying covariance models. *Journal of Business & Economic Statistics*, 39(3):652–668, 2021. [10.1080/07350015.2020.1713795](https://doi.org/10.1080/07350015.2020.1713795).
- D. Pati, A. Bhattacharya, N. Pillai, and D. Dunson. Posterior contraction in sparse bayesian factor models for massive covariance matrices. *The Annals of Statistics*, 42(3):1102–1130, 2014. [10.1214/14-AOS1215](https://doi.org/10.1214/14-AOS1215).
- B. Poignard and J.-D. Fermanian. The finite sample properties of sparse M-estimators with pseudo-observations. *Annals of the Institute of Statistical Mathematics*, 74:1–31, 2022. [10.1007/s10463-021-00785-4](https://doi.org/10.1007/s10463-021-00785-4).
- B. Poignard and Y. Terada. Statistical analysis of sparse approximate factor models. *Electronic Journal of Statistics*, 14(2):3315–3365, 2020. [10.1214/20-EJS1745](https://doi.org/10.1214/20-EJS1745).

- A. Rothman, P. Bickel, E. Levina, and J. Zhu. Penalized profiled semi-parametric estimating functions. *Electronic Journal of Statistics*, 2:494–515, 2008. [10.1214/08-EJS176](https://doi.org/10.1214/08-EJS176).
- J. Stock and M. Watson. Forecasting using principal components from a large number of predictors. *Journal of the American statistical Association*, 97(460):1167–1179, 2002. [10.1198/016214502388618960](https://doi.org/10.1198/016214502388618960).
- Y. Uematsu and T. Yamagata. Estimation of sparsity-induced weak factor models. *Journal of Business & Economic Statistics*, 41(1):213–227, 2023. [10.1080/07350015.2021.2008405](https://doi.org/10.1080/07350015.2021.2008405).
- Z. Wen and W. Yin. A feasible method for optimization with orthogonality constraints. *Mathematical Programming*, 142(1-2):397–434, 2013. [10.1007/s10107-012-0584-1](https://doi.org/10.1007/s10107-012-0584-1).
- M. West. Bayesian factor regression models in the “large p, small n” paradigm. *Bayesian Statistics 7*, in V Lindley, and others (eds):733–742, 2003. [10.1093/oso/9780198526155.003.0053](https://doi.org/10.1093/oso/9780198526155.003.0053).
- C.-H. Zhang. Nearly unbiased variable selection under minimax concave penalty. *The Annals of Statistics*, 38(2):894–942, 2010. [10.1214/09-AOS729](https://doi.org/10.1214/09-AOS729).

Appendix A Preliminary results

In this section, we provide three deviation bounds on the empirical variance-covariance matrix of ϵ_t, F_t and the covariance $\epsilon_t F_t^\top$.

Lemma A.1. *Suppose Assumptions 1–2 of the main text are satisfied. Let $\rho^{-1} = 3r_1^{-1} + 1.5r_2^{-1} + r_3^{-1} + 1$ and assume $\log(p_n)^{6/\rho} = o(n)$. Then, the following bounds are satisfied:*

- (i) $\max_{1 \leq k \leq m, 1 \leq l \leq p_n} \left| \frac{1}{n} \sum_{t=1}^n F_{t,k} \epsilon_{t,l} \right| = O_p(\sqrt{\log(p_n)/n})$.
- (ii) $\max_{1 \leq k, l \leq m} \left| \frac{1}{n} \sum_{t=1}^n F_{t,k} F_{t,l} - \mathbb{E}[F_{t,k} F_{t,l}] \right| = O_p(\sqrt{1/n})$.
- (iii) $\max_{1 \leq k, l \leq p_n} \left| \frac{1}{n} \sum_{t=1}^n \epsilon_{t,k} \epsilon_{t,l} - \Psi_{n,kl} \right| = O_p(\sqrt{\log(p_n)/n})$.

Proof. The proofs of these deviation inequalities follow from Lemma A.3 and Lemma B.1 of [Fan et al. \(2011\)](#). \square

Appendix B Proofs

In this section, we provide the proofs of Theorem 3.1 and Theorem 3.2, where $\hat{\theta}_n$ is defined in (2.1) and $\mathbb{L}_n(\theta) = \sum_{t=1}^n \ell_n(X_t; \theta)$. We will write $\hat{S}_n = n^{-1} \sum_{t=1}^n X_t X_t^\top$.

B.1 Proof of Theorem 3.1

We first provide the proof when $\ell_n(X_t; \theta_n)$ is the Gaussian loss. We then consider the least squares case.

Gaussian loss. Let $\ell_n(X_t; \theta_n) = \text{tr}(X_t X_t^\top \Sigma_n^{-1}) + \log(|\Sigma_n|)$, $\Sigma_n = \Lambda_n \Lambda_n^\top + \Psi_n$. Note that $n^{-1} \sum_{t=1}^n \ell_n(X_t; \theta_n) = \text{tr}(\hat{S}_n \Sigma_n^{-1}) + \log(|\Sigma_n|)$. Define the symmetric positive-definite matrix

$$V_n = \Lambda_n^* R_u^\top + R_u \Lambda_n^{*\top} + R_u R_u^\top + D_u, \quad R_u = (r_{u,1}, \dots, r_{u,p_n})^\top \in \mathbb{R}^{p_n \times m}, \quad D_u \in \mathbb{R}^{p_n \times p_n},$$

with R_u a fixed matrix satisfying $\forall 1 \leq j \leq p_n, \|r_{u,j}\|_2 \leq \kappa < \infty$ and D_u a fixed diagonal matrix with positive and bounded diagonal terms satisfying $\forall 1 \leq k \leq p_n, \kappa^{-2} \leq D_{u,kk} \leq \kappa^2$. Under the sparsity assumption, $\|\Lambda_n^*\|_F = O(s_n^{1/2})$. Define the re-scaled positive-definite and symmetric matrix $U_n = V_n / s_n^{1/2} =: L_{n,u} + R_u R_u^\top / s_n^{1/2} + D_u / s_n^{1/2}$ and let $\Delta_{n,u} = \alpha_n U_n$

with $\alpha_n = p_n \sqrt{s_n \log(p_n)/n} + \sqrt{p_n} A_n$. We aim to prove that for any $\delta > 0$, there exists $C_\delta > 0$ large and finite such that

$$\mathbb{P}(\alpha_n^{-1} \|\widehat{\Sigma}_n - \Sigma_n^*\|_F > C_\delta) < \delta.$$

Define $\mathbb{L}_n^{\text{pen}}(\theta_n) = \mathbb{L}_n(\theta_n) + n \sum_{k=1}^{p_n m} p(|\theta_{n\Lambda, k}|, \gamma_n)$, we have

$$\mathbb{P}(\alpha_n^{-1} \|\widehat{\Sigma}_n - \Sigma_n^*\|_F > C_\delta) \leq \mathbb{P}(\exists U_n \in \mathcal{A}_n : \mathbb{L}_n^{\text{pen}}(\theta_n^* + \text{vec}(\Delta_{n,u})) \geq \mathbb{L}_n^{\text{pen}}(\theta_n^*)), \quad (\text{B.1})$$

with $\mathcal{A}_n := \{U_n : \|\Delta_{n,u}\|_F^2 = \alpha_n^2 C_\delta^2\}$. If the right-hand side of (B.1) is smaller than ϵ , this implies that there is a local minimum in $\{\Sigma_n^* + \Delta_{n,u} : \|\Delta_{n,u}\|_F^2 \leq \alpha_n^2 C_\delta^2\}$ such that $\|\widehat{\Sigma}_n - \Sigma_n^*\|_F = O_p(\alpha_n)$ for n large enough, because $\Sigma_n^* + \Delta_{n,u}$ is positive-definite. Indeed, we have

$$\lambda_{\min}(\Sigma_n^* + \Delta_{n,u}) \geq \lambda_{\min}(\Sigma_n^*) + \lambda_{\min}(\Delta_{n,u}) \geq \lambda_{\min}(\Sigma_n^*) - \|\Delta_{n,u}\|_F > 0,$$

because Σ_n^* is positive-definite by construction and $\|\Delta_{n,u}\|_F = O(\alpha_n) = o(1)$. The following expansion holds:

$$\begin{aligned} & \frac{1}{n} \mathbb{L}_n^{\text{pen}}(\theta_n^* + \text{vec}(\Delta_{n,u})) - \frac{1}{n} \mathbb{L}_n^{\text{pen}}(\theta_n^*) \\ & \geq \text{tr}(\widehat{S}_n(\Sigma_n^* + \Delta_{n,u})^{-1}) + \log |\Sigma_n^* + \Delta_{n,u}| - \text{tr}(\widehat{S}_n(\Sigma_n^*)^{-1}) - \log |\Sigma_n^*| \\ & \quad + \sum_{k \in \mathcal{S}_n} \left(p(|\theta_{n\Lambda}^* + \alpha_n \text{vec}(L_{n,u} + R_u R_u^\top)|, \gamma_n) - p(|\theta_{n\Lambda}^*|, \gamma_n) \right) \\ & = \nabla_{\text{vec}(\Sigma_n)^\top} \frac{1}{n} \mathbb{L}_n(\theta_n^*) \text{vec}(\Delta_{n,u}) + \text{vec}(\Delta_{n,u})^\top \int_0^1 g(v, \Sigma_{n,v}) (1-v) dv \text{vec}(\Delta_{n,u}) \\ & \quad + \sum_{k \in \mathcal{S}_n} \left(\alpha_n \partial_1 p(|\theta_{n\Lambda}^*|, \gamma_n) \text{vec}(L_{n,u} + R_u R_u^\top)_k + \alpha_n^2 \partial_{11}^2 p(|\theta_{n\Lambda}^*|, \gamma_n) \text{vec}(L_{n,u} + R_u R_u^\top)_k^2 \{1 + o(1)\} \right) \\ & =: K_1 + K_2 + K_3, \end{aligned}$$

with $\Sigma_{n,v} = \Sigma_n^* + v \Delta_{n,u}$ and

$$g(v, \Sigma_{n,v}) = \Sigma_{n,v}^{-1} \otimes \Sigma_{n,v}^{-1} \widehat{S}_n \Sigma_{n,v}^{-1} + \Sigma_{n,v}^{-1} \widehat{S}_n \Sigma_{n,v}^{-1} \otimes \Sigma_{n,v}^{-1} - \Sigma_{n,v}^{-1} \otimes \Sigma_{n,v}^{-1},$$

which is obtained by the identification of the Hessian matrix using, e.g., Theorem 18.6 of [Magnus and Neudecker \(2019\)](#). We want to prove

$$\mathbb{P}(\exists U_n \in \mathcal{A}_n : nK_1 + nK_2 + nK_3 \geq 0) < \delta. \quad (\text{B.2})$$

Hereafter, to simplify the notations, we divide by n in (B.2). Take K_1 :

$$K_1 = \text{vec}(\Sigma_n^{*-1}(\Sigma_n^* - \hat{\Sigma}_n)\Sigma_n^{*-1})^\top \text{vec}(\Delta_{n,u}) = \text{tr}((\Sigma_n^* - \hat{\Sigma}_n)\Sigma_n^{*-1}(\Delta_{n,u})\Sigma_n^{*-1}).$$

K_1 can be upper bounded as

$$|K_1| = \left| \sum_{ij} [\Sigma_n^* - \hat{\Sigma}_n]_{ij} (\Sigma_n^{*-1} \Delta_{n,u} \Sigma_n^{*-1})_{ij} \right| \leq p_n \max_{1 \leq ij \leq p_n} |(\hat{\Sigma}_n - \Sigma_n^*)_{ij}| \|\Sigma_n^{*-1}\|_s^2 \|\Delta_{n,u}\|_F.$$

We have the decomposition:

$$\hat{\Sigma}_n - \Sigma_n^* = \Lambda_n^* \hat{S}_{FF} \Lambda_n^{*\top} + \Lambda_n^* \hat{S}_{n, F\epsilon} + \hat{S}_{n, \epsilon F} \Lambda_n^{*\top} + \hat{S}_{n, \epsilon\epsilon} - \Lambda_n^* \Lambda_n^{*\top} - \Psi_n^*,$$

with $\hat{S}_{FF} = n^{-1} \sum_{t=1}^n F_t F_t^\top$, $\hat{S}_{n, F\epsilon} = n^{-1} \sum_{t=1}^n F_t \epsilon_t^\top$, $\hat{S}_{n, \epsilon F} = \hat{S}_{n, F\epsilon}^\top$, $\hat{S}_{n, \epsilon\epsilon} = n^{-1} \sum_{t=1}^n \epsilon_t \epsilon_t^\top$. Now denoting by \mathbf{e}_k the p_n -dimensional zero column vector except for the k -th component being one, we obtain

$$\begin{aligned} & \|\hat{\Sigma}_n - \Sigma_n^*\|_{\max} \\ & \leq 2 \max_{1 \leq k, l \leq p_n} \|\mathbf{e}_k^\top \Lambda_n^* \left(\frac{1}{n} \sum_{t=1}^n F_t \epsilon_t^\top \right) \mathbf{e}_l\|_2 + \max_{1 \leq k, l \leq p_n} \left| \left(\frac{1}{n} \sum_{t=1}^n \epsilon_t \epsilon_t^\top - \Psi_n^* \right)_{kl} \right| + \max_{1 \leq k, l \leq p_n} \|\mathbf{e}_k^\top \Lambda_n^* \left(\frac{1}{n} \sum_{t=1}^n F_t F_t^\top - I_m \right) \Lambda_n^{*\top} \mathbf{e}_l\|_2 \\ & \leq 2 \max_{1 \leq k \leq p_n} \|\lambda_k^*\|_2 \sqrt{m} \max_{1 \leq k \leq m, 1 \leq l \leq p_n} \left| \frac{1}{n} \sum_{t=1}^n F_{t,k} \epsilon_{t,l} \right| + \left\| \frac{1}{n} \sum_{t=1}^n \epsilon_t \epsilon_t^\top - \Psi_n^* \right\|_{\max} + m^2 \|\Lambda_n^*\|_{\max}^2 \left\| \frac{1}{n} \sum_{t=1}^n F_t F_t^\top - \mathbb{E}[F_t F_t^\top] \right\|_{\max}. \end{aligned}$$

Therefore, under Assumption 4, we deduce

$$\begin{aligned} |K_1| & = \left| \sum_{ij} [\Sigma_n^* - \hat{\Sigma}_n]_{ij} (\Sigma_n^{*-1} \Delta_{n,u} \Sigma_n^{*-1})_{ij} \right| \\ & \leq p_n \left(2 \max_{1 \leq k \leq p_n} \|\lambda_k^*\|_2 \sqrt{m} \max_{1 \leq k \leq m, 1 \leq l \leq p_n} \left| \frac{1}{n} \sum_{t=1}^n F_{t,k} \epsilon_{t,l} \right| + \left\| \frac{1}{n} \sum_{t=1}^n \epsilon_t \epsilon_t^\top - \Psi_n^* \right\|_{\max} \right. \\ & \quad \left. + m^2 \|\Lambda_n^*\|_{\max}^2 \left\| \frac{1}{n} \sum_{t=1}^n F_t F_t^\top - \mathbb{E}[F_t F_t^\top] \right\|_{\max} \right) \|\Sigma_n^{*-1}\|_s^2 \|\Delta_{n,u}\|_F \\ & \leq p_n \left(2 \max_{1 \leq k \leq p_n} \|\lambda_k^*\|_2 \sqrt{m} O_p \left(\sqrt{\frac{\log(p_n)}{n}} \right) + O_p \left(\sqrt{\frac{\log(p_n)}{n}} \right) + m^2 \|\Lambda_n^*\|_{\max}^2 O_p \left(\sqrt{\frac{\log(p_n)}{n}} \right) \right) \|\Sigma_n^{*-1}\|_s^2 \|\Delta_{n,u}\|_F, \end{aligned}$$

applying Lemma A.1. Therefore, we obtain $|K_1| \leq O_p(\alpha_n^2 C_\delta)$. As for K_2 , note that

$$\|v \Sigma_n^{*-1} \Delta_{n,u}\|_s \leq \|\Sigma_n^{*-1}\|_s \|\Delta_{n,u}\|_F \leq O(1) C_\delta \alpha_n = o(1).$$

By the expansion $(A + \Delta)^{-1} = \sum_{k=0}^{\infty} (-A^{-1} \Delta)^k A^{-1}$, we write $\Sigma_{n,v} = \Sigma_n^* (I_{p_n} + \Sigma_n^{*-1} v \Delta_{n,u})$

and thus obtain

$$\Sigma_{n,v}^{-1} = (I_{p_n} + \Sigma_n^{*-1} v \Delta_{n,u})^{-1} \Sigma_n^{*-1} = \sum_{k=0}^{\infty} (-\Sigma_n^{*-1} v \Delta_{n,u})^k \Sigma_n^{*-1} \Sigma_n^{*-1} = \Sigma_n^{*-1} - \Sigma_n^{*-1} v \Delta_{n,u} \Sigma_n^{*-1} + \mathcal{R},$$

with $\mathcal{R} = (\Sigma_n^{*-1} v \Delta_{n,u})^2 (I_{p_n} + \Sigma_n^{*-1} v \Delta_{n,u})^{-1} \Sigma_n^{*-1}$. The remainder \mathcal{R} can be bounded as

$$\|\mathcal{R}\|_s \leq \|\Sigma_n^{*-1} \Delta_{n,u}\|_s^2 \|(I_{p_n} + \Sigma_n^{*-1} v \Delta_{n,u})^{-1}\|_s \|\Sigma_n^{*-1}\|_s \leq \frac{\|\Sigma_n^{*-1} \Delta_{n,u}\|_s^2 O(1)}{1 - \|\Sigma_n^{*-1} \Delta_{n,u}\|_s} = o(1).$$

Therefore, we deduce $\Sigma_{n,v}^{-1} = \Sigma_n^{*-1} (I_{p_n} - v \Delta_{n,u} \Sigma_n^{*-1} + o(1))$, and so $\|\Sigma_{n,v}^{-1}\|_s = \underline{\mu} + O_p(\alpha_n)$.

Moreover, since $\|\hat{S}_n - \Sigma_n^*\|_s = O_p(\alpha_n)$, we get

$$\hat{S}_n \Sigma_{n,v}^{-1} = (\hat{S}_n - \Sigma_n^*) \Sigma_{n,v}^{-1} + \Sigma_n^* \Sigma_{n,v}^{-1} = o_p(1) + I_{p_n} + O_p(\alpha_n) = I_{p_n} + o_p(1).$$

So we obtain $g(v, \Sigma_{n,v}) = \Sigma_n^{*-1} \otimes \Sigma_n^{*-1} + O_p(\alpha_n)$. This implies

$$\begin{aligned} K_2 &= \text{vec}(\Delta_{n,u})^\top \int_0^1 \left[\Sigma_n^{*-1} \otimes \Sigma_n^{*-1} + o_p(1) \right] (1-v) dv \text{vec}(\Delta_{n,u}) \\ &\geq \lambda_{\min}(\Sigma_n^{*-1} \otimes \Sigma_n^{*-1}) \|\Delta_{n,u}\|_F^2 / 2 (1 + o_p(1)) = \underline{\mu}^{-2} C_\delta^2 \alpha_n^2 / 2 (1 + o_p(1)). \end{aligned}$$

Finally, we consider the penalty part K_3 . By Assumption 7, we have

$$|K_3| \leq \sqrt{s_n} \alpha_n \max_{1 \leq k \leq p_n m} \{\partial_1 p(|\theta_{n\Lambda}^*|, \gamma_n)\} \|\Delta_{n,u}\|_F + 2\alpha_n^2 \max_{1 \leq k \leq p_n m} \{\partial_{11}^2 p(|\theta_{n\Lambda}^*|, \gamma_n)\} \|\Delta_{n,u}\|_F^2.$$

Therefore, putting the pieces together, for large enough $C_\delta > 0$, we deduce

$$\mathbb{L}_n^{\text{pen}}(\theta_n^* + \text{vec}(\Delta_{n,u})) - \mathbb{L}_n^{\text{pen}}(\theta_n^*) = n \text{vec}(\Delta_{n,u})^\top (\Sigma_n^{*-1} \otimes \Sigma_n^{*-1}) \text{vec}(\Delta_{n,u}) (1 + o_p(1)),$$

which is larger than $n \underline{\mu}^{-2} C_\delta^2 \alpha_n^2 / 2 > 0$. We deduce (B.2) and finally $\|\hat{S}_n - \Sigma_n^*\|_F = O_p(\alpha_n)$.

Least squares loss. We now establish the result when $\ell_n(X_t; \theta_n) = \text{tr}((X_t X_t^\top - \Sigma_n)^2)$. We note that $n^{-1} \sum_{t=1}^n \text{tr}((X_t X_t^\top - \Sigma_n)^2)$, is equivalent to $\|\hat{S}_n - \Sigma\|_F^2$ up to some constant terms that do not depend on Λ_n, Ψ_n . Indeed:

$$\text{tr}((\hat{S}_n - \Sigma)^2) = \text{tr}(\hat{S}_n^\top \hat{S}_n) - \text{tr}(\hat{S}_n^\top \Sigma_n + \Sigma_n^\top \hat{S}_n) + \text{tr}(\Sigma_n^\top \Sigma_n),$$

which is, up to constant terms that do not depend on Σ , equivalent to:

$$\frac{1}{n} \sum_{t=1}^n \text{tr}((X_t X_t^\top - \Sigma_n)^2) = \frac{1}{n} \sum_{t=1}^n \text{tr}((X_t X_t^\top)^\top X_t X_t^\top - (X_t X_t^\top)^\top \Sigma_n - \Sigma_n^\top X_t X_t^\top + \Sigma_n^\top \Sigma_n).$$

Hereafter, we will work with the form $\|\widehat{S}_n - \Sigma_n\|_F^2$ and so we write $\mathbb{L}_n(\theta_n) = \|\widehat{S}_n - \Sigma_n\|_F^2$. Following the same steps and using the same notations as in the Gaussian case, we have the expansion

$$\begin{aligned}
& \frac{1}{n} \mathbb{L}_n^{\text{pen}}(\theta_n^* + \text{vec}(\Delta_{n,u})) - \frac{1}{n} \mathbb{L}_n^{\text{pen}}(\theta_n^*) \\
& \geq \|\widehat{S}_n - (\Sigma_n^* + \Delta_{n,u})\|_F^2 - \|\widehat{S}_n - \Sigma_n^*\|_F^2 \\
& \quad + \sum_{k \in \mathcal{S}_n} \left(p(|\theta_{n\Lambda}^*| + \alpha_n \text{vec}(\Delta_{n,u,\Lambda})|, \gamma_n) - p(|\theta_{n\Lambda}^*|, \gamma_n) \right) \\
& = 2 \text{vec}(\Sigma_n^* - \widehat{S}_n)^\top \text{vec}(\Delta_{n,u}) + \text{vec}(\Delta_{n,u})^\top 2(I_{p_n} \otimes I_{p_n}) \text{vec}(\Delta_{n,u}) \\
& \quad + \sum_{k \in \mathcal{S}_n} \left(\alpha_n \partial_1 p(|\theta_{n\Lambda}^*|, \gamma_n) \text{vec}(L_{n,u})_k + \alpha_n^2 \partial_{11}^2 p(|\theta_{n\Lambda}^*|, \gamma_n) \text{vec}(L_{n,u})_k^2 \{1 + o(1)\} \right) \\
& =: K_1 + K_2 + K_3.
\end{aligned}$$

K_1 can be bounded as

$$|K_1| \leq 2 \left| \sum_{ij} [\Sigma_n^* - \widehat{S}_n]_{ij} \Delta_{n,u} \right| \leq \alpha_n \|\Delta_{n,u}\|_F.$$

We thus get $|K_1| \leq O_p(\alpha_n^2 C_\delta)$. Now, since $\nabla_{\text{vec}(\Sigma_n) \text{vec}(\Sigma_n)^\top}^2 \mathbb{L}_n(\theta_n^*) = I_{p_n} \otimes I_{p_n}$, it implies that $K_2 \geq \|\Delta_{n,u}\|_F^2$. We thus deduce $\|\widehat{\Sigma}_n - \Sigma_n^*\|_F = O_p(\alpha_n)$.

B.2 Proof of Theorem 3.2

Consistency of $\widehat{\theta}_n$. From Theorem 3.1, we have

$$\|\widehat{\Lambda}_n \widehat{\Lambda}_n^\top + \widehat{\Psi}_n - \Sigma_n^*\|_F = O_p(p_n \sqrt{s_n \log(p_n)/n} + \sqrt{p_n} A_n).$$

Define $\alpha_n = \sqrt{p_n} (\sqrt{p_n s_n \log(p_n)/n} + A_n)$. Then, under Assumptions 8–9, by Theorem 1 of Kano (1983), we obtain:

$$\|\widehat{\theta}_n - \theta_n^*\|_\infty = O_p(\alpha_n).$$

Therefore, for any $\delta > 0$, there exists $C_\delta > 0$ such that $\mathbb{P}(\|\widehat{\theta}_n - \theta_n^*\|_2 > C_\delta \sqrt{p_n} \alpha_n) < \delta$. The $\|\cdot\|_\infty$ -consistency of $\widehat{\theta}_n$ follows from the ‘‘strong identifiability’’ property of the factor model defined in Kano (1983): the latter property holds if and only if, for any $\epsilon > 0$, $\exists \delta > 0$ such that if $\|\Sigma_n - \Sigma_n^*\|_{\max} < \delta$, then $\|\Lambda_n - \Lambda_n^*\|_{\max} < \epsilon$ and $\|\Psi_n - \Psi_n^*\|_{\max} < \epsilon$, with $\Sigma_n = \Lambda_n \Lambda_n^\top + \Psi_n$.

The proof of the sparsity property is performed in the same vein as in Lam and Fan

(2009). We first provide the proof for the estimator deduced from the Gaussian loss. The least squares case will follow.

Sparsity property.

Gaussian loss. We consider an estimator $\hat{\theta}_n = (\hat{\theta}_{n\Lambda,1}^\top, \hat{\theta}_{n\Lambda,2}^\top, \hat{\theta}_{n\Psi}^\top)^\top$ of θ_n^* satisfying $\|\hat{\theta}_n - \theta_n^*\|_2 = O_p(\sqrt{p_n}\alpha_n)$. We aim to show

$$\mathbb{L}_n^{\text{pen}}((\hat{\theta}_{n\Lambda,1}^\top, 0^\top, \hat{\theta}_{n\Psi}^\top)^\top) = \min_{\|\hat{\theta}_{n\Lambda,2}\|_2 \leq C\sqrt{p_n}\alpha_n} \mathbb{L}_n^{\text{pen}}((\hat{\theta}_{n\Lambda,1}^\top, \hat{\theta}_{n\Lambda,2}^\top, \hat{\theta}_{n\Psi}^\top)^\top), \quad (\text{B.3})$$

for any constant $C > 0$ with probability tending to one. Let $u_n = C\sqrt{p_n}\alpha_n$. To prove (B.3), it is sufficient to show that for any θ_n such that $\|\theta_n - \theta_n^*\|_2 \leq u_n$, with probability tending to one, we have:

$$\partial_{\theta_{n\Lambda,j}} \mathbb{L}^{\text{pen}}(\theta_n) > 0 \text{ when } 0 < \theta_{n\Lambda,j} < u_n, \quad \partial_{\theta_{n\Lambda,j}} \mathbb{L}^{\text{pen}}(\theta_n) < 0 \text{ when } -u_n < \theta_{n\Lambda,j} < 0,$$

for $j \in \mathcal{S}_n^c$. Using the derivative formulas of Section C of the Appendix, for a minimizer (Λ_n, Ψ_n) , we have:

$$\partial_{\theta_{n\Lambda,j}} \mathbb{L}^{\text{pen}}(\theta_n) = n \, 2 \, \text{vec}(\Sigma_n^{-1}(\Sigma_n - \hat{S}_n)\Sigma_n^{-1}\Lambda_n)_j + n \, \partial_1 p(|\theta_{n\Lambda,j}|, \gamma_n) \, \text{sgn}(\theta_{n\Lambda,j}),$$

where $\text{sgn}(x)$ is the sign of x . We aim to show that the sign of $\partial_{\theta_{n\Lambda,j}} \mathbb{L}^{\text{pen}}(\theta_n)$ depends on $\text{sgn}(\theta_{n\Lambda,j})$ only with probability tending to one: this means that the estimated parameter is at 0, implying $\hat{\theta}_{n\Lambda,j} = 0$ for all $j \in \mathcal{S}_n^c$. First, by Lemma 1 of Lam and Fan (2009), we have

$$\begin{aligned} \text{vec}(\Sigma_n^{-1}(\Sigma_n - \hat{S}_n)\Sigma_n^{-1}\Lambda_n)_j &\leq \|\Sigma_n^{-1}(\Sigma_n - \hat{S}_n)\Sigma_n^{-1}\Lambda_n\|_s \\ &\leq \|\Sigma_n^{-1}\|_s^2 \|\Sigma_n - \hat{S}_n\|_s \|\Lambda_n\|_s \leq O(1) (\|\Sigma_n - \Sigma_n^*\|_s + \|\Sigma_n^* - \hat{S}_n\|_s) (\|\Lambda_n - \Lambda_n^*\|_s + \|\Lambda_n^*\|_s). \end{aligned}$$

Since $\|\Sigma_n^{-1}\|_s^2 \leq \|\Psi_n^{-1}\|_s = O(1)$, we deduce

$$\text{vec}(\Sigma_n^{-1}(\Sigma_n - \hat{S}_n)\Sigma_n^{-1}\Lambda_n)_j \leq O(1) \left\{ O_p(\alpha_n) + O_p\left(p_n \sqrt{\frac{\log(p_n)}{n}}\right) \right\} (O_p(\sqrt{p_n}\alpha_n) + \sqrt{s_n}).$$

Therefore,

$$\begin{aligned} \partial_{\theta_{n\Lambda,j}} \mathbb{L}^{\text{pen}}(\theta_n) &= n \, O_p\left(\sqrt{\frac{p_n^3 s_n \log(p_n)}{n}} + p_n^2 \sqrt{\frac{\log(p_n)}{n}} A_n\right) + n \, \partial_{\Lambda_n,ij} p(|\theta_{n\Lambda,ij}|, \gamma_n) \, \text{sgn}(\theta_{n\Lambda,j}) \\ &= n \, \gamma_n \left\{ O_p(\gamma_n^{-1} \sqrt{\frac{p_n^3 s_n \log(p_n)}{n}} + \gamma_n^{-1} p_n^2 \sqrt{\frac{\log(p_n)}{n}} A_n) + \gamma_n^{-1} \partial_1 p(|\theta_{n\Lambda,j}|, \gamma_n) \, \text{sgn}(\theta_{n\Lambda,j}) \right\}. \end{aligned}$$

Under $\gamma_n^{-1} \sqrt{\frac{p_n^3 s_n \log(p_n)}{n}} \rightarrow 0$, $p_n^2 \sqrt{\log(p_n)} A_n = o(\gamma_n \sqrt{n})$, $\liminf_{n \rightarrow \infty} \liminf_{x \rightarrow 0^+} \gamma_n^{-1} \partial_1 p(x, \gamma_n) > 0$, the sign of $\partial_{\Lambda_n, ij} \mathbb{L}^{\text{pen}}(\theta_n)$ depends on $\text{sgn}(\theta_{n, \Lambda_{ij}})$ with probability tending to one.

Least squares loss. Following the same steps as in the Gaussian loss, for any θ_n such that $\|\theta_n - \theta_n^*\|_2 \leq u_n$ and $u_n = C \sqrt{p_n} \alpha_n$, we show that the sign of $\partial_{\theta_{n, \Lambda, j}} \mathbb{L}^{\text{pen}}(\theta_n)$ depends on $\text{sgn}(\theta_{n, \Lambda, j})$ and $j \in \mathcal{S}_n^c$ only. For a minimizer (Λ_n, Ψ_n) , we have:

$$\partial_{\theta_{n, \Lambda, j}} \mathbb{L}^{\text{pen}}(\theta_n) = n \, 4 \, \text{vec}((\Sigma_n - \widehat{S}_n) \Lambda_n)_j + n \, \partial_1 p(|\theta_{n, \Lambda, j}|, \gamma_n) \, \text{sgn}(\theta_{n, \Lambda, j}),$$

for any $j \in \mathcal{S}_n^c$. The first order term can be bounded as $\text{vec}((\Sigma_n - \widehat{S}_n) \Lambda_n)_j \leq \|\Sigma_n - \widehat{S}_n\|_s \|\Lambda_n\|_s$. Therefore, we deduce

$$\partial_{\theta_{n, \Lambda, j}} \mathbb{L}^{\text{pen}}(\theta_n) = n \, \gamma_n \left\{ O_p \left(\gamma_n^{-1} \sqrt{\frac{p_n^3 s_n \log(p_n)}{n}} + \gamma_n^{-1} p_n A_n \right) + \gamma_n^{-1} \partial_1 p(|\theta_{n, \Lambda, j}|, \gamma_n) \, \text{sgn}(\theta_{n, \Lambda, j}) \right\}.$$

Hence, $\widehat{\theta}_{n, \Lambda, k} = 0$ for any $k \in \mathcal{S}_n^c$ with probability one.

Consistency of the GLS estimator. We now move to the consistency of the GLS estimator \widehat{F}_t , for any fixed $t = 1, \dots, n$. The proof can be done in the same spirit as in [Bai and Liao \(2016\)](#), Theorem 3.1. Based on the factor decomposition $X_t = \Lambda_n^* F_t + \epsilon_t$, for any t , we have

$$\widehat{F}_t - F_t = -(\widehat{\Lambda}_n^\top \widehat{\Psi}_n^{-1} \widehat{\Lambda}_n)^{-1} \widehat{\Lambda}_n^\top \widehat{\Psi}_n^{-1} (\widehat{\Lambda}_n - \Lambda_n^*) F_t + (\widehat{\Lambda}_n^\top \widehat{\Psi}_n^{-1} \widehat{\Lambda}_n)^{-1} \widehat{\Lambda}_n^\top \widehat{\Psi}_n^{-1} \epsilon_t =: M_1 + M_2.$$

We first consider M_1 . Define $\widehat{\xi}_k^{(1)}$ as the k -th column of $\widehat{\Lambda}_n^\top \widehat{\Psi}_n^{-1}$. It can be bounded as

$$\begin{aligned} |M_1| &\leq \|(\widehat{\Lambda}_n^\top \widehat{\Psi}_n^{-1} \widehat{\Lambda}_n)^{-1}\|_s \sqrt{\sum_{k=1}^{p_n} \|\widehat{\xi}_k^{(1)} (\widehat{\lambda}_k - \lambda_k^*)\|_2^2} \|F_t\| \\ &\leq \lambda_{\max}(\widehat{\Psi}_n) \lambda_{\min}(\widehat{\Lambda}_n^\top \widehat{\Lambda}_n)^{-1} O_p(1) \|\widehat{\Lambda}_n - \Lambda_n^*\|_F \|F_t\| \leq O_p(p_n^{-\nu}) O_p(1) \|\widehat{\Lambda}_n - \Lambda_n^*\|_F \|F_t\| = o_p(1), \end{aligned}$$

since $\max_k \|\widehat{\xi}_k^{(1)}\|_2 = O_p(1)$ and under $\lambda_{\min}(\widehat{\Lambda}_n^\top \widehat{\Lambda}_n)^{-1} = O_p(p_n^{-\nu})$, with $1/2 < \nu \leq 1$. As for M_2 , it can be rewritten as

$$M_2 = (\widehat{\Lambda}_n^\top \widehat{\Psi}_n^{-1} \widehat{\Lambda}_n)^{-1} \Lambda_n^{*\top} \Psi_n^{*-1} \epsilon_t + (\widehat{\Lambda}_n^\top \widehat{\Psi}_n^{-1} \widehat{\Lambda}_n)^{-1} (\widehat{\Lambda}_n^\top \widehat{\Psi}_n^{-1} - \Lambda_n^{*\top} \Psi_n^{*-1}) \epsilon_t =: L_1 + L_2.$$

We have

$$\begin{aligned} |L_2| &\leq O_p(p_n^{-\nu}) \|(\widehat{\Lambda}_n^\top \widehat{\Psi}_n^{-1} - \Lambda_n^{*\top} \Psi_n^{*-1}) \epsilon_t\|_F \\ &\leq O_p(p_n^{-\nu}) \left(\|(\widehat{\Lambda}_n^\top - \Lambda_n^*) \widehat{\Psi}_n^{-1} \epsilon_t\|_F + \|\Lambda_n^{*\top} (\widehat{\Psi}_n^{-1} - \Psi_n^{*-1}) \epsilon_t\|_F \right) =: P_1 + P_2. \end{aligned}$$

First, we treat P_1 . Define by $\widehat{v}_{t,k}$ as the k -th entry of $\widehat{\Psi}_n^{-1} \epsilon_t$. Then

$$P_1 \leq O_p(p_n^{-\nu}) \sqrt{\sum_{k=1}^{p_n} \|(\widehat{\lambda}_k - \lambda_k^*) \widehat{v}_{t,k}\|_2^2} = O_p(p_n^{-\nu}) O_p(\sqrt{p_n}) \|\widehat{\Lambda}_n^\top - \Lambda_n^*\|_F = o_p(1).$$

To bound P_2 , first note $P_2 = O_p(p_n^{-\nu}) \|\Lambda_n^{*\top} \widehat{\Psi}_n^{-1} (\Psi_n^* - \widehat{\Psi}_n) \Psi_n^{*-1} \epsilon_t\|_F$. Then define $\widehat{\xi}_k^{(2)}$ as the k -th column of $\Lambda_n^{*\top} \widehat{\Psi}_n^{-1}$ and $v_{t,k}$ the k -th entry of $\Psi_n^{*-1} \epsilon_t$. We obtain

$$\|\Lambda_n^{*\top} (\widehat{\Psi}_n^{-1} - \Psi_n^{*-1}) \epsilon_t\|_F = \sqrt{\sum_{k=1}^{p_n} \|\widehat{\xi}_k^{(2)} (\Psi_{n,kk}^* - \widehat{\Psi}_{n,kk}) v_{t,k}\|_2^2} \leq \sqrt{\sum_{k=1}^{p_n} \|\widehat{\xi}_k^{(2)}\|^2 |v_{t,k}|^2 |\widehat{\Psi}_{n,kk} - \Psi_{n,kk}^*|^2}.$$

Since $\max_k \|\widehat{\xi}_k^{(2)}\|_2 = O_p(1)$ and $\max_k \|v_{t,k}\|_2 = O_p(\log(p_n))$, we deduce

$$\|\Lambda_n^{*\top} (\widehat{\Psi}_n^{-1} - \Psi_n^{*-1}) \epsilon_t\|_F \leq O_p(\log(p_n)) \|\widehat{\Psi}_n - \Psi_n^*\|_F.$$

Therefore, we get

$$P_2 = O_p(p_n^{-\nu}) O_p(\log(p_n)) \|\widehat{\Psi}_n - \Psi_n^*\|_F = o_p(1).$$

Hence, denoting by ξ_k the k -th column of $\Lambda_n^{*\top} \Psi_n^{*-1}$, we can deduce

$$\|\widehat{F}_t - F_t\| \leq O_p(p_n^{-\nu}) \sum_{k=1}^{p_n} \|\epsilon_{t,k} \xi_k\| + o_p(1) = O_p(p_n^{-\nu+1/2}) + o_p(1) = o_p(1).$$

Appendix C Derivative formulas

In this section, to ease the notations, we do not index by n the model parameters, the function $\ell(\cdot; \cdot)$ and the sample variance-covariance \widehat{S} . We provide here the formulas of the first and second derivatives of $\mathbb{L}_n(\cdot)$ with respect to the factor model parameters $\theta = (\theta_\Lambda^\top, \theta_\Psi^\top)$. Although the proofs of Theorem 3.1 and Theorem 3.2 do not require the second and cross-derivatives, it is still of interest to derive these quantities. We will present the derivative formulas when $\mathbb{L}_n(\theta)$ is under the form $\mathbb{L}_n(\theta) = n^{-1} \sum_{t=1}^n \ell(X_t; \theta)$.

Hereafter, $\theta = (\theta_\Lambda^\top, \theta_\Psi^\top)^\top$, where $\theta_\Lambda = \text{vec}(\Lambda)$ and $\Sigma = \Lambda\Lambda^\top + \Psi$, $\Lambda \in \mathbb{R}^{p \times m}$, $\Psi \in \mathbb{R}^{p \times p}$. As for the Ψ parameter, we will provide the first derivative with respect $\theta_\Psi = \text{vec}(\Psi) \in \mathbb{R}^{p^2}$, i.e., for any $\mathbb{R}^{p \times p}$ matrix, and with respect to $\theta_\Psi = \text{diag}(\Psi) = (\sigma^2, \dots, \sigma_p^2)^\top \in \mathbb{R}^p$, i.e., when accounting for the diagonal restriction on Ψ . The second order derivative will be provided with respect to $\theta_\Psi = \text{vec}(\Psi) \in \mathbb{R}^{p^2}$ and $\theta_\Psi = (\sigma^2, \dots, \sigma_p^2)^\top \in \mathbb{R}^p$.

C.1 Gaussian loss function

The Gaussian loss $\mathbb{L}_n(\theta) = n^{-1} \sum_{t=1}^n \ell(X_t; \theta)$, with $\ell(X_t; \theta) = \text{tr}((X_t X_t^\top) \Sigma^{-1}) + \log(|\Sigma|)$, can be written as $\mathbb{L}_n(\theta) = \text{tr}(\hat{S} \Sigma^{-1}) + \log(|\Sigma|)$, $\hat{S} = n^{-1} \sum_{t=1}^n X_t X_t^\top$, which will be used hereafter. The first differential of $\mathbb{L}_n(\cdot)$ is:

$$d\mathbb{L}_n(\theta) = \text{tr}(-\hat{S} \Sigma^{-1} (d\Sigma) \Sigma^{-1} + \Sigma^{-1} (d\Sigma)) =: \text{tr}(V(d\Sigma)), \quad V = \Sigma^{-1} - \Sigma^{-1} \hat{S} \Sigma^{-1}.$$

The differential of V is:

$$dV = -\Sigma^{-1} (d\Sigma) \Sigma^{-1} + \Sigma^{-1} (d\Sigma) \Sigma^{-1} \hat{S} \Sigma^{-1} + \Sigma^{-1} \hat{S} \Sigma^{-1} (d\Sigma) \Sigma^{-1} = \Sigma^{-1} (d\Sigma) \Sigma^{-1} - \Sigma^{-1} (d\Sigma) V - V (d\Sigma) \Sigma^{-1}.$$

The second order differential of $\mathbb{L}_n(\cdot)$ becomes:

$$d^2 \mathbb{L}_n(\theta) = \text{tr}((dV)(d\Sigma) + V(d^2 \Sigma)) = \text{tr}(\Sigma^{-1} (d\Sigma) \Sigma^{-1} (d\Sigma)) - 2 \text{tr}(\Sigma^{-1} (d\Sigma) V (d\Sigma)) + \text{tr}(V(d^2 \Sigma)).$$

Here, $d\Sigma = (d\Lambda)\Lambda^\top + \Lambda(d\Lambda)^\top + d\Psi$, $d^2 \Sigma = 2(d\Lambda)(d\Lambda)^\top$, since Λ and Ψ are both linear in the parameters, so that $d^2 \Lambda$ and $d^2 \Psi$ are both zero. We deduce that the first differential of $\mathbb{L}_n(\cdot)$ is $d\mathbb{L}_n(\theta) = 2 \text{tr}(\Lambda^\top V(d\Lambda)) + \text{tr}(V(d\Psi))$, and the second order differential is

$$\begin{aligned} d^2 \mathbb{L}_n(\theta) &= \text{tr}(\Sigma^{-1} (d\Sigma) \Sigma^{-1} (d\Sigma)) - 2 \text{tr}(\Sigma^{-1} (d\Sigma) V (d\Sigma)) + \text{tr}(V(d^2 \Sigma)) \\ &= \text{tr}(\Sigma^{-1} (d\Sigma) \Sigma^{-1} (d\Sigma)) - 2 \text{tr}(\Sigma^{-1} (d\Sigma) V (d\Sigma)) + 2 \text{tr}(V(d\Lambda)(d\Lambda)^\top). \end{aligned}$$

Let us explicit the expression $(d\Sigma) \Sigma^{-1} (d\Sigma)$:

$$\begin{aligned} (d\Sigma) \Sigma^{-1} (d\Sigma) &= [(d\Lambda)\Lambda^\top + \Lambda(d\Lambda)^\top + d\Psi] \Sigma^{-1} [(d\Lambda)\Lambda^\top + \Lambda(d\Lambda)^\top + d\Psi] \\ &= (d\Lambda)\Lambda^\top \Sigma^{-1} (d\Lambda)\Lambda^\top + (d\Lambda)\Lambda^\top \Sigma^{-1} \Lambda(d\Lambda)^\top + (d\Lambda)\Lambda^\top \Sigma^{-1} (d\Psi) + \Lambda(d\Lambda)^\top \Sigma^{-1} (d\Lambda)\Lambda^\top \\ &\quad + \Lambda(d\Lambda)^\top \Sigma^{-1} \Lambda(d\Lambda)^\top + \Lambda(d\Lambda)^\top \Sigma^{-1} (d\Psi) + (d\Psi) \Sigma^{-1} (d\Lambda)\Lambda^\top + (d\Psi) \Sigma^{-1} \Lambda(d\Lambda)^\top + (d\Psi) \Sigma^{-1} (d\Psi). \end{aligned}$$

By the properties of the trace operator:

$$\begin{aligned} \text{tr}((\mathbf{d}\Sigma)\Sigma^{-1}(\mathbf{d}\Sigma)V) &= 2 \text{tr}(\Lambda^\top V(\mathbf{d}\Lambda)\Lambda^\top \Sigma^{-1}(\mathbf{d}\Lambda)) + \text{tr}(\Lambda^\top \Sigma^{-1}\Lambda(\mathbf{d}\Lambda)^\top V(\mathbf{d}\Lambda)) \\ &+ \text{tr}(\Lambda^\top V\Lambda(\mathbf{d}\Lambda)^\top \Sigma^{-1}(\mathbf{d}\Lambda)) + 2 \text{tr}(V(\mathbf{d}\Lambda)\Lambda^\top \Sigma^{-1}(\mathbf{d}\Psi)) + 2 \text{tr}(\Sigma^{-1}(\mathbf{d}\Lambda)\Lambda^\top V(\mathbf{d}\Psi)) \\ &+ \text{tr}((\mathbf{d}\Psi)\Sigma^{-1}(\mathbf{d}\Psi)V), \end{aligned}$$

and

$$\begin{aligned} \text{tr}((\mathbf{d}\Sigma)\Sigma^{-1}(\mathbf{d}\Sigma)\Sigma^{-1}) &= 2 \text{tr}(\Lambda^\top \Sigma^{-1}(\mathbf{d}\Lambda)\Lambda^\top \Sigma^{-1}(\mathbf{d}\Lambda)) \\ &+ 2 \text{tr}(\Lambda^\top \Sigma^{-1}\Lambda(\mathbf{d}\Lambda)^\top \Sigma^{-1}(\mathbf{d}\Lambda)) + 4 \text{tr}(\Sigma^{-1}(\mathbf{d}\Lambda)\Lambda^\top \Sigma^{-1}(\mathbf{d}\Psi)) + \text{tr}((\mathbf{d}\Psi)\Sigma^{-1}(\mathbf{d}\Psi)\Sigma^{-1}). \end{aligned}$$

We thus deduce:

$$\begin{aligned} \mathbf{d}^2\mathbb{L}_n(\theta) &= 2 \text{tr}(\Lambda^\top \Sigma^{-1}(\mathbf{d}\Lambda)\Lambda^\top \Sigma^{-1}(\mathbf{d}\Lambda)) - 4 \text{tr}(\Lambda^\top V(\mathbf{d}\Lambda)\Lambda^\top \Sigma^{-1}(\mathbf{d}\Lambda)) \\ &- 2 \text{tr}(\Lambda^\top \Sigma^{-1}\Lambda(\mathbf{d}\Lambda)^\top V(\mathbf{d}\Lambda)) + 2 \text{tr}((\mathbf{d}\Lambda)^\top V(\mathbf{d}\Lambda)) + 2 \text{tr}(\Lambda^\top \Sigma^{-1}\Lambda(\mathbf{d}\Lambda)^\top \Sigma^{-1}(\mathbf{d}\Lambda)) \\ &- 2 \text{tr}(\Lambda^\top V\Lambda(\mathbf{d}\Lambda)^\top \Sigma^{-1}(\mathbf{d}\Lambda)) + 4 \text{tr}(\Sigma^{-1}\Lambda(\mathbf{d}\Lambda)^\top \Sigma^{-1}(\mathbf{d}\Psi)) - 4 \text{tr}(\Sigma^{-1}\Lambda(\mathbf{d}\Lambda)^\top V(\mathbf{d}\Psi)) \\ &- 4 \text{tr}(V\Lambda(\mathbf{d}\Lambda)^\top \Sigma^{-1}(\mathbf{d}\Psi)) + \text{tr}(\Sigma^{-1}(\mathbf{d}\Psi)\Sigma^{-1}(\mathbf{d}\Psi)) - 2 \text{tr}(\Sigma^{-1}(\mathbf{d}\Psi)V(\mathbf{d}\Psi)) \\ &= \begin{pmatrix} \mathbf{d}\text{vec}(\Lambda) \\ \mathbf{d}\text{vec}(\Psi) \end{pmatrix}^\top \begin{pmatrix} H_{\Lambda\Lambda} & H_{\Lambda\Psi} \\ H_{\Psi\Lambda} & H_{\Psi\Psi} \end{pmatrix} \begin{pmatrix} \mathbf{d}\text{vec}(\Lambda) \\ \mathbf{d}\text{vec}(\Psi) \end{pmatrix}. \end{aligned}$$

Note that the following relationships hold, for any matrices A, B with suitable dimensions, by the formulas for the identification of the Hessian in Theorem 18.6 of [Magnus and Neudecker \(2019\)](#), we have:

$$\begin{aligned} \text{tr}(A(\mathbf{d}\Lambda)^\top B(\mathbf{d}\Lambda)) &= (\mathbf{d}\text{vec}(\Lambda))^\top \left[\frac{1}{2}(A^\top \otimes B) + (A \otimes B^\top) \right] \mathbf{d}\text{vec}(\Lambda), \\ \text{tr}(A(\mathbf{d}\Lambda)B(\mathbf{d}\Lambda)) &= (\mathbf{d}\text{vec}(\Lambda))^\top \left[\frac{1}{2}K_{mp}((A^\top \otimes B) + (B^\top \otimes A)) \right] \mathbf{d}\text{vec}(\Lambda), \\ \text{tr}(A(\mathbf{d}\Lambda)^\top B(\mathbf{d}\Psi)) &= (\mathbf{d}\text{vec}(\Psi))^\top \left[\frac{1}{2}(A^\top \otimes B) + (A \otimes B^\top) \right] \mathbf{d}\text{vec}(\Lambda), \\ \text{tr}(A(\mathbf{d}\Psi)^\top B(\mathbf{d}\Psi)) &= (\mathbf{d}\text{vec}(\Psi))^\top \left[\frac{1}{2}(A^\top \otimes B) + (A \otimes B^\top) \right] \mathbf{d}\text{vec}(\Psi). \end{aligned}$$

Then we can write $\mathbf{d}^2\mathbb{L}_n(\theta) = \sum_{k=1}^4 P_k$, with

$$\begin{aligned} P_1 &= -2 \operatorname{tr}(\Lambda^\top \Sigma^{-1} \Lambda (\mathbf{d}\Lambda)^\top V (\mathbf{d}\Lambda)) + 2 \operatorname{tr}((\mathbf{d}\Lambda)^\top V (\mathbf{d}\Lambda)) \\ &\quad + 2 \operatorname{tr}(\Lambda^\top \Sigma^{-1} \Lambda (\mathbf{d}\Lambda)^\top \Sigma^{-1} (\mathbf{d}\Lambda)) - 2 \operatorname{tr}(\Lambda^\top V \Lambda (\mathbf{d}\Lambda)^\top \Sigma^{-1} (\mathbf{d}\Lambda)) \\ &= 2(\mathbf{d}\operatorname{vec}(\Lambda))^\top \left[-(\Lambda^\top \Sigma^{-1} \otimes V) + (I_m \otimes V) + (\Lambda^\top \Sigma^{-1} \Lambda \otimes \Sigma^{-1}) - (\Lambda^\top V \Lambda \otimes \Sigma^{-1}) \right] \mathbf{d}\operatorname{vec}(\Lambda), \end{aligned}$$

$$\begin{aligned} P_2 &= 2 \operatorname{tr}(\Lambda^\top \Sigma^{-1} (\mathbf{d}\Lambda) \Lambda^\top \Sigma^{-1} (\mathbf{d}\Lambda)) - 4 \operatorname{tr}(\Lambda^\top V (\mathbf{d}\Lambda) \Lambda^\top \Sigma^{-1} (\mathbf{d}\Lambda)) \\ &= 2(\mathbf{d}\operatorname{vec}(\Lambda))^\top K_{mp} \left[(\Sigma^{-1} \Lambda \otimes \Lambda^\top \Sigma^{-1}) - (V \Lambda \otimes \Lambda^\top \Sigma^{-1}) - (\Sigma^{-1} \Lambda \otimes \Lambda^\top V) \right] \mathbf{d}\operatorname{vec}(\Lambda), \end{aligned}$$

$$\begin{aligned} P_3 &= 4 \operatorname{tr}(\Sigma^{-1} \Lambda (\mathbf{d}\Lambda)^\top \Sigma^{-1} (\mathbf{d}\Psi)) - 4 \operatorname{tr}(\Sigma^{-1} \Lambda (\mathbf{d}\Lambda)^\top V (\mathbf{d}\Psi)) - 4 \operatorname{tr}(V \Lambda (\mathbf{d}\Lambda)^\top \Sigma^{-1} (\mathbf{d}\Psi)) \\ &= 4(\mathbf{d}\operatorname{vec}(\Psi))^\top \left[(\Sigma^{-1} \Lambda \otimes \Sigma^{-1}) - (\Sigma^{-1} \Lambda \otimes V) - (V \Lambda \otimes \Sigma^{-1}) \right] \mathbf{d}\operatorname{vec}(\Psi), \end{aligned}$$

and

$$P_4 = \operatorname{tr}(\Sigma^{-1} (\mathbf{d}\Psi) \Sigma^{-1} (\mathbf{d}\Psi)) - 2 \operatorname{tr}(\Sigma^{-1} (\mathbf{d}\Psi) V (\mathbf{d}\Psi)) = 4(\mathbf{d}\operatorname{vec}(\Psi))^\top \left[(\Sigma^{-1} \otimes \Sigma^{-1}) - 2(\Sigma^{-1} \otimes V) \right] \mathbf{d}\operatorname{vec}(\Psi).$$

Therefore, $\nabla_\Lambda \mathbb{L}_n(\theta) = 2\Sigma^{-1}(\Sigma - \hat{S})\Sigma^{-1}\Lambda$, $\nabla_\Psi \mathbb{L}_n(\theta) = \Sigma^{-1}(\Sigma - \hat{S})\Sigma^{-1}$, so that in vector form:

$$\nabla_{\theta_\Lambda} \mathbb{L}_n(\theta) = 2 \operatorname{vec}(\Sigma^{-1}(\Sigma - \hat{S})\Sigma^{-1}\Lambda) \in \mathbb{R}^{pm}, \quad \nabla_{\theta_\Psi} \mathbb{L}_n(\theta) = \operatorname{vec}(\Sigma^{-1}(\Sigma - \hat{S})\Sigma^{-1}) \in \mathbb{R}^{p^2}.$$

As for the Hessian matrix, we have:

$$\begin{aligned} \nabla_{\theta_\Lambda \theta_\Lambda^\top}^2 \mathbb{L}_n(\theta) &= 2 K_{mp} (\Sigma^{-1} \Lambda \otimes \Lambda^\top \Sigma^{-1}) - 2 K_{mp} \left[(V \Lambda \otimes \Lambda^\top \Sigma^{-1}) + (\Sigma^{-1} \Lambda \otimes \Lambda^\top V) \right] \\ &\quad + 2 \left[-(\Lambda^\top \Sigma^{-1} \Lambda \otimes V) + (I_m \otimes V) + (\Lambda^\top \Sigma^{-1} \Lambda \otimes \Sigma^{-1}) - (\Lambda^\top V \Lambda \otimes \Sigma^{-1}) \right], \end{aligned}$$

and $\nabla_{\theta_\Psi \theta_\Psi^\top}^2 \mathbb{L}_n(\theta) = (\Sigma^{-1} \otimes \Sigma^{-1}) - 2(\Sigma^{-1} \otimes V) \in \mathbb{R}^{p^2 \times p^2}$. Finally, the cross-derivative is

$$\nabla_{\theta_\Psi \theta_\Lambda^\top}^2 \mathbb{L}_n(\theta) = 2 \left[(\Sigma^{-1} \Lambda \otimes \Sigma^{-1}) - (\Sigma^{-1} \Lambda \otimes V) - (V \Lambda \otimes \Sigma^{-1}) \right], \quad (\nabla_{\theta_\Psi \theta_\Lambda^\top}^2 \mathbb{L}_n(\theta))^\top = \nabla_{\theta_\Lambda \theta_\Psi^\top}^2 \mathbb{L}_n(\theta).$$

Under the diagonality constraint w.r.t. Ψ , i.e., Ψ is diagonal with $\theta_\Psi = (\sigma_1^2, \dots, \sigma_p^2)^\top \in \mathbb{R}^p$, the gradient becomes $\nabla_{\theta_\Psi} \mathbb{L}_n(\theta) = \operatorname{diag}(I_p \odot (\Sigma^{-1}(\Sigma - \hat{S})\Sigma^{-1}))$. To take the diagonality constraint w.r.t. Ψ in the Hessian matrix, we introduce the selection matrix $D_p^* \in \mathbb{R}^{p^2 \times p}$, defined by $D_p^* = \sum_{k=1}^p (e_k \otimes e_k) e_k^\top$, with $e_k \in \mathbb{R}^p$ the p -dimensional vector with zero entries

only, excluding the k -th element which is 1. Therefore, the Hessian matrix becomes:

$$\nabla_{\theta_\Psi \theta_\Lambda}^2 \mathbb{L}_n(\theta) = D_p^{*\top} [(\Sigma^{-1} \otimes \Sigma^{-1}) - 2(\Sigma^{-1} \otimes V)] D_p^* \in \mathbb{R}^{p \times p},$$

and $\nabla_{\theta_\Psi \theta_\Lambda}^2 \mathbb{L}_n(\theta) = 2 D_p^{*\top} [(\Sigma^{-1} \Lambda \otimes \Sigma^{-1}) - (\Sigma^{-1} \Lambda \otimes V) - (V \Lambda \otimes \Sigma^{-1})]$.

C.2 Least squares loss function

Following the preliminary remark in the proof of Theorem 3.1, least squares case, $\mathbb{L}_n(\theta) = n^{-1} \sum_{t=1}^n \text{tr}((X_t X_t^\top - \Sigma)^2)$ is equivalent to $\|\hat{S} - \Sigma\|_F^2$, up to some constant terms that do not depend on Λ, Ψ . Hereafter, to obtain our derivatives, we work with $\mathbb{L}_n(\theta) = \|\hat{S} - \Sigma\|_F^2$. The first differential of $\mathbb{L}_n(\cdot)$ is:

$$d\mathbb{L}_n(\cdot) = \text{tr}(2\Sigma(d\Sigma) - 2\hat{S}(d\Sigma)) =: \text{tr}(V(d\Sigma)), \quad V = 2(\Sigma - \hat{S}).$$

Since $dV = 2d\Sigma$, the second order differential becomes:

$$d^2\mathbb{L}_n(\theta) = 2 \text{tr}((d\Sigma)(d\Sigma)) + \text{tr}(V(d^2\Sigma)), \quad d\Sigma = (d\Lambda)\Lambda^\top + \Lambda(d\Lambda)^\top + d\Psi, \quad d^2\Sigma = 2(d\Lambda)(d\Lambda)^\top.$$

We have:

$$\begin{aligned} (d\Sigma)(d\Sigma) &= ((d\Lambda)\Lambda^\top + \Lambda(d\Lambda)^\top + d\Psi)((d\Lambda)\Lambda^\top + \Lambda(d\Lambda)^\top + d\Psi) \\ &= (d\Lambda)\Lambda^\top(d\Lambda)\Lambda^\top + (d\Lambda)\Lambda^\top\Lambda(d\Lambda) + (d\Lambda)\Lambda^\top(d\Psi) + \Lambda(d\Lambda)^\top(d\Lambda)\Lambda^\top + \Lambda(d\Lambda)^\top\Lambda(d\Lambda) \\ &\quad + \Lambda(d\Lambda)^\top(d\Psi) + (d\Psi)(d\Lambda)\Lambda^\top + (d\Psi)\Lambda(d\Lambda)^\top + (d\Psi)(d\Psi). \end{aligned}$$

We then deduce:

$$d\mathbb{L}_n(\theta) = \text{tr}(V((d\Lambda)\Lambda^\top + \Lambda(d\Lambda)^\top + d\Psi)) = 2 \text{tr}(\Lambda^\top V(d\Lambda)) + \text{tr}(V(d\Psi)),$$

and

$$\begin{aligned} d^2\mathbb{L}_n(\theta) &= 2 \text{tr}(((d\Lambda)\Lambda^\top + \Lambda(d\Lambda)^\top + d\Psi)((d\Lambda)\Lambda^\top + \Lambda(d\Lambda)^\top + d\Psi)) + 2 \text{tr}(V(d\Lambda)(d\Lambda)^\top) \\ &= 4 \text{tr}(\Lambda^\top(d\Lambda)\Lambda^\top(d\Lambda)) + 4 \text{tr}(\Lambda^\top\Lambda(d\Lambda)^\top(d\Lambda)) + 2 \text{tr}((d\Lambda)^\top V(d\Lambda)) + 8 \text{tr}(\Lambda(d\Lambda)^\top(d\Psi)) + 2 \text{tr}((d\Psi)(d\Psi)) \\ &= \begin{pmatrix} d\text{vec}(\Lambda) \\ d\text{vec}(\Psi) \end{pmatrix}^\top \begin{pmatrix} H_{\Lambda\Lambda} & H_{\Lambda\Psi} \\ H_{\Psi\Lambda} & H_{\Psi\Psi} \end{pmatrix} \begin{pmatrix} d\text{vec}(\Lambda) \\ d\text{vec}(\Psi) \end{pmatrix} \end{aligned}$$

Following the same steps as in the Gaussian loss function, the gradients are $\nabla_{\Lambda} \mathbb{L}_n(\theta) = 4(\Sigma - \hat{S})\Lambda$, $\nabla_{\Psi} \mathbb{L}_n(\theta) = 2(\Sigma - \hat{S})$, i.e., $\nabla_{\theta_{\Lambda}} \mathbb{L}_n(\theta) = 4 \text{vec}((\Sigma - \hat{S})\Lambda)$, $\nabla_{\theta_{\Psi}} \mathbb{L}_n(\theta) = 2 \text{vec}(\Sigma - \hat{S})$. The Hessian matrix is:

$$\nabla_{\theta_{\Lambda} \theta_{\Lambda}^{\top}}^2 \mathbb{L}_n(\theta) = 4K_{m,p}(\Lambda \otimes \Lambda^{\top}) + 4(\Lambda^{\top} \Lambda \otimes I_p) + 2(I_m \otimes V), \quad \nabla_{\theta_{\Psi} \theta_{\Psi}^{\top}}^2 \mathbb{L}_n(\theta) = 2(I_p \otimes I_p),$$

and the cross-derivative is given by $\nabla_{\theta_{\Psi} \theta_{\Lambda}^{\top}}^2 \mathbb{L}_n(\theta) = 4(\Lambda \otimes I_p)$, $(\nabla_{\theta_{\Psi} \theta_{\Lambda}^{\top}}^2 \mathbb{L}_n(\theta))^{\top} = \nabla_{\theta_{\Lambda} \theta_{\Psi}^{\top}}^2 \mathbb{L}_n(\theta)$. Under the diagonality constraint w.r.t. Ψ , i.e., Ψ is diagonal with $\theta_{\Psi} = (\sigma_1^2, \dots, \sigma_p^2)^{\top} \in \mathbb{R}^p$, the gradient becomes $\nabla_{\theta_{\Psi}} \mathbb{L}_n(\theta) = 2 \text{diag}(I_p \odot (\Sigma - \hat{S}))$ and the Hessian becomes $\nabla_{\theta_{\Psi} \theta_{\Psi}^{\top}}^2 \mathbb{L}_n(\theta) = 2D_p^{*\top}(I_p \otimes I_p)D_p^*$ and $\nabla_{\theta_{\Psi} \theta_{\Lambda}^{\top}}^2 \mathbb{L}_n(\theta) = 4D_p^{*\top}(\Lambda \otimes I_p)$.

Appendix D Implementations

In this section, we discuss the computational issues to estimate the penalized factor model. To ease the notations, the factor model parameters and the variables relating to the dimension are not indexed by n . The code was implemented on Matlab and run on Intel(R) Xeon(R) Gold 6242R CPU, 3.10GHz, with Installed RAM 128 GB. We make the code for the sparse factor model and corresponding simulated experiments publicly available in the following Github repository: <https://github.com/Benjamin-Poignard/sparse-factor-models>

D.1 Algorithm

Recall that $\theta = (\theta_{\Lambda}^{\top}, \theta_{\Psi}^{\top})^{\top}$, where $\theta_{\Lambda} = \text{vec}(\Lambda)$ and $\Sigma = \Lambda\Lambda^{\top} + \Psi$, $\Lambda \in \mathbb{R}^{p \times m}$, $\Psi \in \mathbb{R}^{p \times p}$. The penalized problem is solved according to the following steps:

Step 1: Initialization.

- (i) Solve $\hat{\theta} := (\hat{\theta}_{\Lambda}^{\top}, \hat{\theta}_{\Psi}^{\top})^{\top} = \arg \min_{\theta \in \Theta_{\text{ic}}} \mathbb{L}_n(\theta)$, with Θ_{ic} the parameter set $\Theta_{\text{ic}} = \{\theta = (\theta_{\Lambda}^{\top}, \theta_{\Psi}^{\top}) : \Lambda^{\top} \Psi^{-1} \Lambda / p \text{ diagonal, } \Psi \text{ diagonal}\}$. This estimator corresponds to the strict factor model estimator of [Bai and Li \(2012\)](#) and is obtained by the EM algorithm following their Section 8.
- (ii) For a given γ_n , set a grid size K . $\forall 1 \leq l \leq K$, solve

$$Q^l = \arg \min_{Q: Q^{\top} Q = I_m} \left\{ \sum_{k=1}^{pm} p(|\theta_{Q,k}|, \gamma_n) \right\}, \text{ where } \theta_Q = \text{vec}(\hat{\Lambda} Q),$$

with $\hat{\Lambda}$ the estimator of step (i). The problem is solved using the algorithm developed by [Wen and Yin \(2013\)](#) for minimization problems subject to orthogonal constraints. The optimal value \tilde{Q}_{γ_n} is set as the argument $Q^l, 1 \leq l \leq K$, providing the minimum value of the previous loss.

Step 2: Iteration. Set $\theta_{\Psi^{(0)}} = \text{diag}(\hat{\Psi}), \hat{\Psi}$ obtained in **Step 1**. For each given γ_n , repeat (i)-(ii) until convergence:

- (i) Solve $\Lambda_{(k+1)} = \arg \min_{\theta_{\Lambda}} \{ \mathbb{L}_n((\theta_{\Lambda}^{\top}, \theta_{\Psi^{(k)}}^{\top})^{\top}) + \sum_{k=1}^{pm} p(|\theta_{\Lambda,k}|, \gamma_n) \}$. The penalized problem is optimized by a gradient descent algorithm based on the updating formulas of Section 4.2 in [Loh and Wainwright \(2015\)](#). The initial value for Λ is set as the rotated matrix $\hat{\Lambda} \tilde{Q}_{\gamma_n}$, with $\hat{\Lambda}$ obtained in **Step 1**.
- (ii) Solve $\theta_{\Psi^{(k+1)}} = \arg \min_{\theta_{\Psi}} \mathbb{L}_n((\theta_{\Lambda^{(k+1)}}^{\top}, \theta_{\Psi}^{\top})^{\top})$ s.t. Ψ diagonal. The problem is optimized by the EM algorithm.

Step 1 is crucial to provide suitable starting values for Λ . In our experiments, we set $K = 200$. We set $a_{\text{mcp}} = 3.7$ for the SCAD and $b_{\text{mcp}} = 3.5$ for the MCP.

D.2 Selection of γ_n

The tuning parameter γ_n controls the model complexity and must be calibrated for each penalty. The selection strategy depends on the nature of the data: i.i.d. or dependent. In the case of i.i.d. data, we employ a 5-fold cross-validation procedure, in the same spirit as in, e.g., Section 7.10 of [Hastie et al. \(2009\)](#). To be specific, we divide the data into 5 disjoint subgroups of roughly the same size - the so-called folds - and denote the index of observations in the k -th fold by $T_k, 1 \leq k \leq 5$ and the size of the k -th fold by n_k . The 5-fold cross-validation score is defined as $\text{CV}(\gamma_n) = \sum_{k=1}^5 \left\{ n_k^{-1} \sum_{i \in T_k} \ell(X_i; \hat{\theta}_{-k}(\gamma_n)) \right\}$, with $n_k^{-1} \sum_{i \in T_k} \ell(X_i; \hat{\theta}_{-k}(\gamma_n))$ the non-penalized loss evaluated over the k -th fold T_k of size n_k , which serves as the test set, and $\hat{\theta}_{-k}(\gamma_n)$ is the estimator of the factor model based on the sample $(\bigcup_{k=1}^5 T_k) \setminus T_k$ - the training set -. The optimal tuning parameter γ_n^* is then selected according to: $\gamma_n^* = \arg \min_{\gamma_n} \text{CV}(\gamma_n)$. Then, γ_n^* is used to obtain the final estimate over the whole data $(\bigcup_{k=1}^5 T_k)$. Here, the minimization of the cross-validation score is performed over a $\{c\sqrt{\log(\text{dim})/n}\}$, with c a user-specified grid of values, set, e.g., as $c = 0.001, 0.005, 0.01, 0.015, \dots, 4$, and dim the problem dimension, i.e., $\text{dim} = pm$. The cross-validation score also be performed over c simply.

Several procedures have been proposed to take into account the dependency among observations, but there is no consensual approach. Based on thorough simulated and real

data experiments, [Cerqueira et al. \(2020\)](#) concluded that good estimation performances are obtained by the "blocked" cross-validation when the process is stationary; under non-stationary time series, the most accurate estimations are produced by "out-of-sample" methods, where the last part of the data is used for testing. In our experiments, we follow the out-of-sample approach for cross-validation. To be specific, we split the full sample into training and test sets. The training sample corresponds to the first 75% of the entire sample and the test sample to the last 25%. For given values of γ_n , we estimate the sparse factor model in the training set and then compute the loss function in the test set using the estimator computed on the training set. This procedure is repeated for all the γ_n candidates and we select the one minimizing the loss. Then, we estimate the model over the full sample using the optimal γ_n . Formally, the procedure is as follows: divide the data into two sets, the training set and test set; define the cross-validation score as $\text{CV}(\gamma_n) = n_{\text{oos}}^{-1} \sum_{i \in T_{\text{oos}}} \ell(X_i; \hat{\theta}_{\text{in}}(\gamma_n))$, where n_{oos} is the size of the test set, T_{oos} is the index of observations in the test set, and $\hat{\theta}_{\text{in}}(\gamma_n)$ is the factor model estimator based on the training set with regularization parameter γ_n . The optimal regularization parameter γ_n^* is then selected according to: $\gamma_n^* = \arg \min_{\gamma_n} \text{CV}(\gamma_n)$. Then, γ_n^* is used to obtain the final estimator over the whole data. Here, the minimization of the cross-validation score is performed over $\{c\sqrt{\log(\text{dim})/n}\}$, with c a grid of values as in the i.i.d. case.

Appendix E Competing models

E.1 DCC model

Rather than a direct specification of the variance-covariance matrix process (Σ_t) of the time series (r_t), an alternative approach is to split the task into two parts: individual conditional volatility dynamics on one side, and conditional correlation dynamics on the other side. The most commonly used correlation process is the Dynamic Conditional Correlation (DCC) of [Engle \(2002\)](#). In its BEKK form, the general DCC model is specified as: $r_t = \Sigma_t^{1/2} \eta_t$, with $\Sigma_t := \mathbb{E}[r_t r_t^\top | \mathcal{F}_{t-1}]$ positive definite, where:

$$\Sigma_t = D_t R_t D_t, \quad R_t = Q_t^{\star-1/2} Q_t Q_t^{\star-1/2}, \quad Q_t = \Omega + \sum_{k=1}^q M_k Q_{t-k} M_k^\top + \sum_{l=1}^r W_l u_{t-l} u_{t-l}^\top W_l^\top,$$

where $D_t = \text{diag}(\sqrt{h_{t,1}}, \sqrt{h_{t,2}}, \dots, \sqrt{h_{t,p}})$ with $(h_{t,j})$ the univariate conditional variance dynamic of the j -th component, $u_t = (u_{t,1}, \dots, u_{t,p})$ with $u_{t,j} = r_{t,j} / \sqrt{h_{t,j}}$, $Q_t = [q_{t,uv}]$, $Q_t^\star = \text{diag}(q_{t,11}, q_{t,22}, \dots, q_{t,pp})$. \mathcal{F}_{t-1} is the sigma field generated by the past information of the p -dimensional process $(r_t)_{t \in \mathbb{Z}}$ until (but including) time $t - 1$. The model is

parameterized by some deterministic matrices $(M_k)_{k=1,\dots,q}$, $(W_l)_{l=1,\dots,r}$ and a positive definite $p \times p$ matrix Ω . In the original DCC of [Engle \(2002\)](#), the process (Q_t) is defined by $Q_t = \Omega^* + \sum_{k=1}^q B_k \odot Q_{t-k} + \sum_{l=1}^r A_l \odot u_{t-l} u_{t-l}^\top$, where the deterministic matrices $(B_k)_{k=1,\dots,q}$ and $(A_l)_{l=1,\dots,r}$ are positive semi-definite. Since the number of parameters of the latter models is of order $O(p^2)$, our applications are restricted to scalar B_k 's and A_l , say b_k, a_l , and we work with $q = r = 1$. Moreover, we employ a correlation targeting strategy, that is we replace Ω^* by $(1 - a_1 - b_1)\bar{Q}$ with \bar{Q} the sample covariance of the standardized returns u_t . We specify a GARCH(1,1) model for each individual conditional variance dynamic h_{tj} . The estimation is performed by a standard two-step Gaussian QML for the MSCI and S&P 100 portfolio. For the S&P 500 portfolio, we employ the composite likelihood method proposed in [Pakel et al. \(2021\)](#) to fix the bias problem caused by the two-step quasi likelihood estimation and to make the likelihood decomposition plausible for large vectors. The composite likelihood method consists of averaging the second step likelihood (correlation part) over 2×2 correlation-based likelihoods. To be precise, using the n -sample of observations, the second step composite likelihood becomes:

$$\mathbb{L}_{2n}(a_1, b_1) = \frac{1}{n} \sum_{t=1}^n \sum_{l=1}^L \left[\log(|R_t^{(l)}|) + u_t^{(l)\top} (R_t^{(l)})^{-1} u_t^{(l)} \right],$$

where $R_t^{(l)}$ is the 2×2 correlation matrix with l corresponding to a pre-specified pair of indices in $\{1, \dots, p\}$, $u_t^{(l)}$ is a 2×1 sub-vector of the standardized residuals u_t , with k selecting the pre-specified pair of indices in $\{1, \dots, p\}$. There are several ways of selecting the pairs: every distinct pair of the assets, i.e., $u_t^{(1)} = (u_{t,1}, u_{t,2})^\top$, $u_t^{(2)} = (u_{t,1}, u_{t,3})^\top, \dots, u_t^{p(p-1)/2} = (u_{t,p-1}, u_{t,p})^\top$, so that $L = p(p-1)/2$ in $L_{2n}(a_1, b_1)$; or contiguous overlapping pairs, i.e., $u_t^{(1)} = (u_{t,1}, u_{t,2})^\top$, $u_t^{(2)} = (u_{t,2}, u_{t,3})^\top, \dots, u_t^{(p-1)} = (u_{t,p-1}, u_{t,p})^\top$ so that $L = p-1$. We use the contiguous overlapping pairs for computation gains, where the complexity is $O(p)$, in contrast to the $O(p^2)$ complexity if $L = p(p-2)/2$: this pair construction is the 2MSCLE method of [Pakel et al. \(2021\)](#).

E.2 Sparse approximate factor model

Based on the same factor model decomposition $X_t = \Lambda F_t + \epsilon_t$, rather than assuming sparsity w.r.t. Λ , [Bai and Liao \(2016\)](#) assume a non-diagonal but sparse Ψ . Assuming bounded eigenvalues for Ψ and under the constraint for identification $\Lambda^\top \Psi^{-1} \Lambda$ diagonal, [Bai and Liao \(2016\)](#) consider the joint estimation of (Λ, Ψ) by Gaussian QML with adaptive-LASSO penalization w.r.t. Ψ : this is the sparse approximate factor model (SAFM) estimator. In all our applications, we employ the Matlab code of [Bai and Liao](#)

(2016) which solves the SAFM by the EM algorithm: the code can be downloaded in <https://econweb.rutgers.edu/y11114/papers/factor3/factor3.html>. The initial values $(\hat{\Lambda}_{\text{init}}, \hat{\Psi}_{\text{init}})$ are set the Gaussian QML estimators of Bai and Li (2012) with $\hat{\Psi}_{\text{init}}$ diagonal. We implemented the adaptive LASSO where the selection of the tuning parameter γ_n follows from same method as in Subsection D.2 in the time series case. The macroeconomic data used in Section 5.2 can be retrieved from the aforementioned website.